

# Ozone pollution may limit the benefits of irrigation to wheat productivity in India

Gabriella Everett<sup>1</sup>, Øivind Hodnebrog<sup>2</sup>, Madhoolika Agrawal<sup>3</sup>, Durgesh Singh Yadav<sup>4</sup>, Connie O'Neill<sup>5</sup>, Chubamenla Jamir<sup>6</sup>, Jo Cook<sup>1,5</sup>, Pritha Pande<sup>1</sup>, Sam Bland<sup>5</sup>, Lisa Emberson<sup>1\*</sup>

<sup>1</sup>Department of Environment and Geography, University of York, York, UK- YO10 5DD.

<sup>2</sup>CICERO Center for International Climate Research – Oslo, 0318, Oslo, Norway

<sup>3</sup>Department of Botany, Institute of Science, Banaras Hindu University, Varanasi 221005, India.

<sup>4</sup>Department of Botany, Government Raza P.G. College, Rampur, U.P. 244901, India.

<sup>5</sup>Stockholm Environment Institute, University of York, York, UK- YO10 5DD.

<sup>6</sup>Climate Studies and Knowledge Solutions Centre, Kohima, Nagaland, India.

*Correspondence to:* Lisa Emberson (l.emberson@york.ac.uk)

**Abstract.** Ground level ozone (O<sub>3</sub>) pollution, heat and water stress are recognised as key abiotic stresses which threaten the ability of wheat yields to meet the growing demand for food production in India. The magnitude and interplay of O<sub>3</sub> and water-stress effects are tightly coupled via stomatal conductance and the transpiration pathway. Existing modelling methods that assess stress response as a function of O<sub>3</sub>- and water vapour-stomatal flux are applied to assess O<sub>3</sub>'s role in limiting productivity afforded by irrigation. We investigate the effect of these stresses on grain yield of older (HUW-234) vs recently released (HD-3118) Indian wheat cultivars under recent past and future climates and O<sub>3</sub> precursor emission profiles (using RCP4.5 and RCP8.5 scenarios). Water-stress in rainfed conditions was modelled to analyse the trade-off between O<sub>3</sub>-induced vs. water-stress-induced yield loss to quantify the extent to which water-stress mitigates O<sub>3</sub> stress via reduced stomatal conductance. Under rainfed conditions for the years 1996-2005, the mean water-stress-induced and O<sub>3</sub>-induced yield loss for HUW-234 was 13.3% and 0.6% respectively. The latter was a significant decrease from the mean O<sub>3</sub>-induced yield loss of 10.6% modelled under irrigated conditions (i.e. no water stress). Similarly, under RCP4.5 and RCP8.5 scenarios for the mid-century, water-stress induced yield losses under rainfed conditions were 10.1% and 20.0%, while mean O<sub>3</sub>-induced yield losses were only 1.0% and 0.1% respectively. Under irrigation, O<sub>3</sub>-induced yield losses increased to 18.5% and 13.7%, suggesting that O<sub>3</sub> stress will negate the beneficial effects of irrigation. The cultivar HD-3118 suffered on average 0.2% greater O<sub>3</sub> relative yield loss (O<sub>3</sub>.RYL) than HUW-234 across all scenarios. The O<sub>3</sub>.RYL increased with climate change under the RCP4.5 scenario by 7.9% and RCP8.5 by 3.0% compared to the recent past climate. Together these findings suggest that O<sub>3</sub> may continue to substantially limit the productivity benefits of the use of modern cultivars bred for high gas exchange grown under irrigated conditions in India.

## 1 Introduction

Wheat is a vital crop for India's economy and food security; India is the second largest wheat producer in the world and most of its population gains >50% of their calorific intake from this staple grain (Tripathi and Mishra, 2017). With India's population of 1.4 billion growing at a rate of 2.23% per year (UNDESA, 2022), wheat will play a major role in ensuring food supply meets the growing demand (Tripathi and Mishra, 2017). However, India's croplands are exposed to particularly high O<sub>3</sub> concentrations ([O<sub>3</sub>]) with hotspots occurring across the Indo-Gangetic Plains (IGP) (Roy et al., 2008). The 8-hour daily mean O<sub>3</sub> concentrations often reach up to 100 ppb in hotspots during the Rabi crop growing season (October to April) and are therefore a significant threat to India's wheat productivity (Roy et al., 2009). Currently, there are no air quality standards in India to protect crops from surface O<sub>3</sub>, and emissions of O<sub>3</sub> precursors are forecast to continue to rise well into the 21<sup>st</sup> century, driven by persistent growth in industries, including mining and petroleum industries, vehicular traffic and agricultural activities (Ghude et al., 2014; Sharma et al., 2019; Yadav et al., 2019). Ozone distribution varies spatially and temporally but the IGP often experiences high levels due to the long-distance transport of O<sub>3</sub> and its precursors from urban, industrial or power generation centres located across northern India (Singh and Agrawal, 2017).

Ozone damages crops when it diffuses into the intracellular airspace of the leaf via the stomata which triggers a cascade of metabolic and physiological responses resulting in reduced carbon assimilation, premature leaf senescence and visible injury. Together, these effects can lead to reductions in overall yield and quality (Emberson et al., 2018). Since O<sub>3</sub> damage relies on stomatal O<sub>3</sub> flux (i.e., O<sub>3</sub> dose), the scale of damage caused by ambient [O<sub>3</sub>] varies with stomatal conductance. Stomatal conductance is determined in the short-term, by environmental factors that trigger the closure of the stomata, and in the long term, by adaptations to climate change i.e., reduced stomatal density (Emberson et al., 2018). Two other factors also influence a crop's vulnerability to O<sub>3</sub> dose; its detoxification ability and the signal transduction pathway, which regulates the response of cells to the increased oxidative load caused by O<sub>3</sub> (Ainsworth et al., 2008; Kangasjärvi et al., 2005).

It is widely acknowledged that stress conditions including elevated levels of carbon dioxide (CO<sub>2</sub>), heat and water vapour pressure deficit (VPD) and soil water deficit (all of which may be associated with climate change) decrease stomatal conductance, thus reducing O<sub>3</sub> flux in wheat and potentially ameliorating O<sub>3</sub> damage to the photosynthetic apparatus (Feng et al., 2008). In addition, several studies have found modern cultivars are more O<sub>3</sub>-sensitive due to selection for enhanced gas exchange, which could counteract their natural adaptation of lower stomatal conductance resulting from the changing climate. Pleijel et al. (2006) and Yadav et al. (2020) observed greater O<sub>3</sub>-related yield loss in a modern wheat cultivar, HD-3118, bred for a higher yield than HUW-234, which was attributed to the cultivar's higher stomatal density and conductance. Climate change is expected to increase the use of drought-resistant cultivars which can maintain higher stomatal conductance under drought conditions, this will likely increase crop sensitivity to O<sub>3</sub> (Emberson et al., 2018). Eliminating the use of cultivars with higher stomatal conductance is unlikely to improve productivity because, on a broader scale, yield losses due to water stress outweigh those from O<sub>3</sub> (Emberson et al., 2018). However, in major wheat-producing states like Uttar Pradesh, where irrigation

64 is widespread (Zaveri and Lobell, 2019) yield losses due to O<sub>3</sub> may outweigh those due to water stress, hence the use of  
65 cultivars with a lower stomatal conductance may be beneficial.

66 Khan and Soja (2003) found that well-irrigated wheat plants (i.e. with a 75% soil water capacity (SWC)) suffered grain yield  
67 losses of up to 39% when exposed to accumulated O<sub>3</sub> concentrations over a threshold of 40 ppb (AOT40) of ~25ppm/h. Under  
68 severe moisture deficit (35% SWC), no O<sub>3</sub>-related yield loss was observed as O<sub>3</sub> uptake was reduced by up to 90%. However,  
69 the grain yield of water-stressed wheat was significantly less than well-watered wheat. In a similar study by Harmens et al.  
70 (2019) on wheat in Africa, grain yield loss due to O<sub>3</sub> exposure was greater in well-watered plants than in crops that received  
71 reduced irrigation suggesting controlled irrigation as a management tool to reduce O<sub>3</sub> impact. Whilst drought reduces yields  
72 at all stages of development, drought stress during anthesis and grain-filling cause the greatest yield reductions (Farooq et al.,  
73 2014). Additionally, anthesis and grain filling is when wheat is most sensitive to [O<sub>3</sub>] and is the period of time when the [O<sub>3</sub>]  
74 are highest during the Indian growing season (Gelang et al., 2000; Pleijel et al., 1998; Rathore et al., 2023). Several  
75 experimental studies have investigated the interaction between O<sub>3</sub> and drought stress in wheat. While some studies have  
76 observed no significant interactions between increased [O<sub>3</sub>] and water stress (Broberg et al., 2023; Fangmeier et al., 1994),  
77 others have observed an interaction. Ghosh et al., (2020) observed an additive effect of O<sub>3</sub> and drought stress, with a greater  
78 reduction in grain yield when both stressors occurred simultaneously due to the reduction in nutrient uptake and assimilation.  
79 As a result of these contrasting findings, it is evident the trade-offs between O<sub>3</sub> exposure and water stress require further study.

80 Irrigation has the potential to maximise O<sub>3</sub>-stress by providing conditions likely to enhance stomatal conductance such as  
81 plentiful soil and leaf water, transpirational cooling and low leaf-to-air VPD. Irrigation is widespread across the IGP,  
82 particularly in the states of Punjab, Haryana and Uttar Pradesh; the area irrigated as a percentage of the total area of wheat was  
83 99.1%, 99.9% and 99% respectively in 2018-19 (Ministry of Agriculture & Farmers Welfare, 2022), which means that current  
84 wheat crop management practices are likely to enhance sensitivity to O<sub>3</sub>. Modifying irrigation practices has been suggested as  
85 a strategy to reduce O<sub>3</sub> damage, but caution is needed to avoid introducing water stress, which could also negatively affect  
86 yield (Harmens et al., 2019; Teixeira et al., 2011). Irrigation has additional benefits and has often been implemented to offset  
87 heat-related yield losses which occur when temperatures exceed 35°C (Zaveri and Lobell, 2019). However, studies suggest  
88 that sustainable use of India's future groundwater availability with current irrigation practices would mitigate less than 10%  
89 of the climate change impact on crop yield (Fishman, 2018). Additionally, water for irrigation purposes is limited; for example,  
90 Zaveri et al. (2016) found Uttar Pradesh will lack scope for further increasing irrigation as groundwater depletion escalates  
91 due to climate change and increased unsustainable water demand. With irrigation accounting for up to 90% of India's total  
92 water demand, water efficiency in agriculture is a priority in the IGP to achieve better environmental and economic  
93 performance (Fischer et al., 2007; Wada et al., 2013). Here, we explore the interplay between O<sub>3</sub>- and water-stressed induced  
94 yield losses which will help inform whether water efficiencies could also provide some benefits in terms of the decreased  
95 sensitivity of staple crops to O<sub>3</sub>.

96 There have been an increasing number of studies exploring the effect of O<sub>3</sub> on wheat yields using a cumulative stomatal O<sub>3</sub>  
97 flux metric (POD<sub>Y</sub>; phytotoxic O<sub>3</sub> dose over a flux threshold Y) which accounts for the stomatal response to environmental

conditions and plant growth stages that alter O<sub>3</sub> uptake. By comparison, concentration-based exposure metrics such as AOT40 only account for atmospheric [O<sub>3</sub>] which may be decoupled from O<sub>3</sub> uptake under environmental conditions that limit stomatal conductance; they also omit O<sub>3</sub> below 40 ppb which are known to be capable of causing damage (CLRTAP, 2017; Emberson et al., 2018). Mills et al. (2018a) estimated an O<sub>3</sub>-induced yield loss that incorporated the effects of irrigation to be in the range of 15-20% for wheat growing in Uttar Pradesh between 2010-2012 using POD<sub>3</sub>IAM (POD above 3nmol m<sup>-2</sup>s<sup>-1</sup>, parameterised for integrated assessment modelling) (CLRTAP, 2017). This parameterisation was based on European wheat cultivars and a broad-scale assessment of India's wheat growing season with the POD<sub>3</sub>IAM metric being applied according to the formulations of the Deposition of Ozone for Stomatal Exchange (DO<sub>3</sub>SE) model (Büker et al., 2012; CLRTAP, 2017; Emberson et al., 2000a, 2018). An alternative metric used in estimations of stomatal O<sub>3</sub> flux effects on crops is POD<sub>6</sub>SPEC, which is the species-specific phytotoxic O<sub>3</sub> dose above 6 nmol m<sup>-2</sup> s<sup>-1</sup>. This metric is better suited for local-regional risk assessments (CLRTAP, 2017).

Application of the stomatal O<sub>3</sub> flux method allows exploration of the relative effects of both O<sub>3</sub> and water stress on yield since the DO<sub>3</sub>SE model also estimates water vapour fluxes from which potential and actual evapotranspiration can be calculated (Büker et al., 2012). In this study, we parameterise the DO<sub>3</sub>SE 3.1.0 version model for two late-sown Indian wheat cultivars for the estimation of POD<sub>6</sub>SPEC metric. We apply the Weather Research and Forecasting model with Chemistry (WRF-Chem) (Grell et al., 2005) to obtain [O<sub>3</sub>] and climate variable data for Varanasi, Uttar Pradesh. We compare O<sub>3</sub> effect yield losses (using the wheat grain yield flux-effect relationship (CLRTAP, 2017) with yield losses due to water stress based on yield responses to the ratio of actual vs potential evapotranspiration (cf. FAO (2012)). This modelling set-up allows us to explore the relative magnitude of yield losses from O<sub>3</sub> and water stress; how these are likely to change in the future and the relative sensitivities of older vs more recently released Indian cultivars to damage from O<sub>3</sub> pollution.

## 2 Methods

For this study, Varanasi was selected as the study area due to (i) its location in the important wheat-growing IGP and, (ii) the availability of observed crop and O<sub>3</sub> data.

### 2.1 Experimental data

Experimental data from 2016-2018 were obtained for two late sown Indian spring wheat (*Triticum aestivum* L.) cultivars grown at the Botanical Garden, Banaras Hindu University (BHU), Varanasi (25°16' N, 82°59' E; 81.0m above sea level). HUW-234 (released in 1986 by BHU, Varanasi) and HD-3118 (released in 2014 by IARI, New Delhi) were selected based on their heat tolerance and extensive cultivation in the North East Plain Zone of India (Joshi et al., 2007; Yadav et al., 2019). The recently released cultivar, HD-3118 is more high-yielding (6.64 tons ha<sup>-1</sup>) compared to HUW-234 (4.5–5 tons ha<sup>-1</sup>), most likely due to its enhanced capacity for gas exchange. This enhanced capacity for gas exchange is the likely reason for the HD-3118 cultivar having a greater sensitivity to O<sub>3</sub> than the HUW-234 cultivar (Yadav et al., 2020).

129 **2.2 Modelled data**

130 Hourly meteorological and O<sub>3</sub> data for the Varanasi grid box (45 km x 45 km horizontal resolution) were obtained by running  
131 WRF-Chem v.3.8.1 for years 1996-2005 (considered the ‘recent past’ climate) and 2046-2055 using both RCP4.5 and RCP8.5  
132 climate scenarios. The 45 km resolution model domain is the same as in Daloz et al. (2021), and the meteorological initial and  
133 boundary conditions come from global climate model simulations with the Community Earth System Model (CESM) v.1.0.4  
134 (Gent et al., 2011), documented in Hodnebrog et al. (2019). The WRF-Chem simulations are set up with the RADM2 gas-  
135 phase chemistry scheme (Stockwell et al., 1990) and O<sub>3</sub> precursor emissions are from Lamarque et al. (2010) for the historical  
136 period and from Lamarque et al. (2011) for the future RCPs. Global mean CO<sub>2</sub> mixing ratios (ppm) for 1996-2005 were  
137 obtained from NASA (using Tans and Conway (no date) for 1983-2003 and Conway (no date) for 2004-2007). For future  
138 scenarios, RCP4.5 and RCP8.5 [CO<sub>2</sub>] for 2046-2055 were acquired (Meinshausen et al., 2011). WRF-Chem with the RADM2  
139 chemical mechanism has been found to reproduce diurnal average O<sub>3</sub> over India in February-May relatively well, while  
140 noontime O<sub>3</sub> concentrations show considerable differences between simulations with various emission inventories (Sharma et  
141 al., 2017).

142  
143 The RCP climate scenarios are selected to provide a range of climate and pollution futures for India from which a consequent  
144 range in yield responses can be estimated. RCPs are possible greenhouse gas (GHG) emission pathways designed to aid  
145 research into climate change impacts (Riahi et al., 2011). RCP8.5 is a very high baseline, representing the highest GHG  
146 emission pathway in a ‘business as usual’ scenario resulting in a radiative forcing of 8.5 Wm<sup>-2</sup> at the close of the 21<sup>st</sup> century;  
147 equivalent to 1370 ppm [CO<sub>2</sub>] (He and Zhou, 2015; Riahi et al., 2011). RCP4.5 is a medium stabilisation scenario where global  
148 climate policy values the role of natural carbon sequestration and land use, resulting in a radiative forcing target of 4.5 Wm<sup>-2</sup>  
149 (650ppm [CO<sub>2</sub>] equivalent) for 2100 (Riahi et al., 2011; van Vuuren et al., 2011).

150 These data provided input to the DO<sub>3</sub>SE model which was used to simulate stomatal O<sub>3</sub> flux values and water stress  
151 characteristics for the two cultivars for each year. The modelled climate, O<sub>3</sub> and CO<sub>2</sub> data for the recent past climate and  
152 both RCP scenarios are summarised in Table 1. The modelled temperature data are on average 1.3°C warmer in the RCP4.5  
153 scenario and 1.9°C warmer in the RCP8.5 scenario than the recent past modelled climate.

154 **Table 1: Modelled climate, [O<sub>3</sub>] and [CO<sub>2</sub>] data for the Varanasi grid box, used for the recent past climate and both future RCP**  
155 **scenarios (expressed as the range of 24-hour mean values, value in brackets indicates mean). The length of growing season is shown**  
156 **in days over two years and can be visualised in Fig. 2.**

Parameter	Recent past climate (1996-2005)	RCP4.5 (2046-2055)	RCP8.5 (2046-2055)
Temperature (°C )	17.4-20.6 (18.9)	19.1-21.3 (20.2)	19.6-21.8 (20.8)
VPD (hPa)	8.3-14.4 (11.0)	12.5-17.5 (14.5)	11.1-18.1 (15.1)

Precipitation (total over growing season; mm)	72.4-393.4 (235.5)	35.1-184.4 (101.7)	0.93-234.0 (92.5)
[O <sub>3</sub> ] (24 hour mean; ppb)	47.1-50.6 (48.6)	57.9-62.2 (60.5)	54.6-63.0 (59.7)
[CO <sub>2</sub> ] (ppm)	362.6-379.5 (370.7)	476.3-498.5 (487.6)	518.6-570.5 (543.9)
Growing season (Days over 2 years)	339-468	339-466	339-473

### 2.3 Model formulation - O<sub>3</sub> induced yield loss estimates

The DO<sub>3</sub>SE 3.1.0 version model (<https://www.sei.org/projects-and-tools/tools/do3se-deposition-ozone-stomatal-exchange/>) was used to estimate stomatal O<sub>3</sub> flux and subsequent O<sub>3</sub>-induced yield loss for wheat. DO<sub>3</sub>SE is a dry deposition model which takes into account the influence of climatic, soil and plant factors on stomatal conductance to estimate stomatal O<sub>3</sub> flux and determine the accumulated stomatal O<sub>3</sub> uptake during a specified growth period; POD<sub>Y</sub> (CLRTAP, 2017). The stomatal conductance ( $g_{sto}$ ) multiplicative algorithm Eq. (1) used in DO<sub>3</sub>SE estimates hourly  $g_{sto}$  to O<sub>3</sub> by modifying a species-specific maximum  $g_{sto}$  ( $g_{max}$ ) according to environmental variables and is described in Emberson et al. (2000a, b).

$$g_{sto} = g_{max} \times [\min(f_{phen}, f_{O_3})] \times f_{light} \times \max\{f_{min}, (f_{temp} \times f_{VPD} \times f_{sw})\} \quad [1]$$

where  $g_{sto}$  and  $g_{max}$  are expressed as mmol O<sub>3</sub> m<sup>-2</sup> PLA s<sup>-1</sup>. The factors  $f_{phen}$ ,  $f_{O_3}$ ,  $f_{light}$ ,  $f_{temp}$ ,  $f_{VPD}$ ,  $f_{sw}$  and  $f_{min}$  represent the influence of phenology, [O<sub>3</sub>], light, air temperature, VPD, soil water potential and minimum  $g_{sto}$  and are expressed in relative terms as a proportion of  $g_{max}$  (so have a value between 0-1). Functions describing these factors for environmental conditions are described in CLRTAP (2017) based on European wheat varieties; for  $f_{sw}$  (and to simulate  $g_{sto}$  for rainfed wheat) we assume a linear relationship between a relative  $g_{sto}$  of 1 and  $f_{min}$  at soil water potentials (SW) of -0.3 and -1.1 MPa (Ali et al., 1999; Morgan, 1984). To simulate the  $g_{sto}$  of irrigated wheat we simply assume that  $f_{sw}$  is always equal to 1.

Stomatal O<sub>3</sub> flux ( $F_{st}$ ; nmol m<sup>-2</sup> PLA s<sup>-1</sup>) was calculated using Eq. (2).

$$F_{st} = c(zi) \times g_{sto} \times \frac{rc}{(rb+rc)} \quad [2]$$

where  $c(zi)$  is [O<sub>3</sub>] at the top of the canopy height  $i$  (m),  $rc$  and  $rb$  represent leaf surface and quasi-laminar leaf boundary layer resistances respectively, based on leaf dimension and wind speed (CLRTAP, 2017).

The species-specific POD<sub>Y</sub> (POD<sub>Y</sub>SPEC) is estimated for the wheat accumulation period according to Eq. (3).

$$POD_{Y}SPEC = \sum \left[ (F_{st} - Y) \times \left( \frac{3600}{10^6} \right) \right] \quad [3]$$

where  $Y$  (nmol O<sub>3</sub> m<sup>-2</sup> PLA s<sup>-1</sup>) is subtracted from  $F_{st}$  (in nmol m<sup>-2</sup> PLA s<sup>-1</sup>) when  $F_{st} > Y$ , during daylight hours; this  $Y$  value represents the assumed detoxification capacity of wheat to O<sub>3</sub> flux. The value is then converted to hourly fluxes by multiplying by 3600 and to mmol by dividing by 10<sup>6</sup> to give  $POD_{Y}SPEC$  in mmol O<sub>3</sub> m<sup>-2</sup> PLA (CLRTAP, 2017). A  $Y$  value of 6 nmol m<sup>-2</sup>

180 <sup>2</sup> PLA s<sup>-1</sup> was used based on values for European wheat (CLRTAP, 2017). The resulting *POD<sub>6</sub>SPEC* values were used to  
 181 estimate the percentage grain yield (relative to 100% grain yield under pre-industrial O<sub>3</sub> conditions) based on the dose-response  
 182 relationship in Eq. (4).

$$183 \quad \%Grain\ Yield = 100.3 - (3.85 \times POD_6SPEC) \quad [4]$$

184 The relationship in Eq. (4) is taken from CLRTAP (2017) where relative grain yields from 5 wheat cultivars in 4 European  
 185 countries were regressed against the *POD<sub>6</sub>SPEC* value.

## 186 **2.4 Model formulation - water stress induced yield losses**

187 The DO<sub>3</sub>SE 3.1.0 model was also used to model the effect of water stress on yield through the provision of estimates of  
 188 potential (*ET<sub>m</sub>*) and actual (*ET<sub>a</sub>*) evapotranspiration following the DO<sub>3</sub>SE model algorithms used to estimate soil-plant-  
 189 atmosphere cycling of water described in B  ker et al. (2012). These DO<sub>3</sub>SE algorithms essentially estimate the total loss of  
 190 soil water through *ET<sub>a</sub>* (and the equivalent *ET<sub>m</sub>*) using the method of Shuttleworth and Wallace (1985) modified to incorporate  
 191 the atmospheric, boundary layer and stomatal resistances to water vapour flux as calculated within DO<sub>3</sub>SE. Resistances are  
 192 scaled from leaf to canopy using LAI and upscaling methods described in B  ker et al. (2012). LAI is modelled to vary over  
 193 the course of the wheat growing season between a value of 0 and 3.5 m<sup>2</sup>/m<sup>2</sup> (consistent with average maximum LAI values  
 194 frequently found across the IGP region as observed from satellite data (Nigam et al., 2017). The DO<sub>3</sub>SE soil moisture module  
 195 was developed based on the Penman-Monteith model of actual evapotranspiration (*E<sub>t</sub>*), which is described in Eq. (5) (B  ker  
 196 et al., 2012; Monteith, 1965; Shuttleworth and Wallace, 1985):

$$197 \quad E_t = \frac{\Delta (\Phi n - G) + \rho_a c_p \left( \frac{D}{R_{bH_2O}} \right)}{\lambda \left\{ \Delta + \gamma \left( 1 + \frac{R_{stoH_2O}}{R_{bH_2O}} \right) \right\}} \quad [5]$$

198 where  $\Delta$  is the slope of the relationship between the saturation vapour pressure and temperature,  $\Phi n$  is the net radiation at the  
 199 top of the canopy,  $G$  is the soil surface heat flux,  $\rho_a$  is the air density,  $c_p$  is the specific heat of air,  $D$  is the vapour pressure  
 200 deficit of air,  $R_{bH_2O}$  is the canopy boundary layer resistance to water vapour exchange,  $R_{stoH_2O}$  is the stomatal canopy  
 201 resistance to the transfer of water vapour (the inverse of stomatal conductance to water vapour),  $\gamma$  is the psychrometric constant,  
 202 and  $\lambda$  is the latent heat of vaporisation.

203 The effect of *ET<sub>a</sub>* (and hence water-stress) on wheat yield was estimated according to the relationship between relative yield  
 204 and the corresponding relative evapotranspiration (*Et*) described in Doorenbos and Kassam (1979) for spring wheat. When a  
 205 crop is not water-stressed, *ET<sub>a</sub>* is equal to *ET<sub>m</sub>* however in drought conditions, *ET<sub>a</sub>* < *ET<sub>m</sub>* (Yao, 1974). The *ET<sub>a</sub>* and *ET<sub>m</sub>* values  
 206 produced by DO<sub>3</sub>SE were used in Eq. (6).

$$207 \quad 1 - \frac{Y_a}{Y_m} = K_y \left( 1 - \frac{ET_a}{ET_m} \right) \quad [6]$$

208 where  $Y_a$  is the actual relative grain yield and  $Y_m$  is the potential relative grain yield.  $K_y$  is the crop-specific yield response  
 209 factor assumed to be 1.15 for the whole growing season, in accordance with the value for spring wheat from the FAO (Steduto  
 210 et al., 2012).

211 **2.5 Model parameterisation**

212 The DO<sub>3</sub>SE model was parameterised for the HD-3118 and HUW-234 cultivars by (Yadav et al. (2021) using data from a  
 213 series of O<sub>3</sub> exposure experiments at the Banaras Hindu University, Varanasi, Uttar Pradesh. For this study, we use the same  
 214 parameterisation except for the  $f_{phen}$  term (which we allow to vary as a function of effective temperature sum (ETS) during  
 215 the growing season) and the inclusion of the  $f_{O_3}$  term (which accounts for O<sub>3</sub> inducing early onset senescence). The  
 216 parameterisations used for both cultivars are given in Table 2.

217  
 218 **Table 2: Parameterisation of the DO<sub>3</sub>SE model for POD<sub>6</sub>SPEC for wheat flag leaves for Indian bread wheat (*Triticum aestivum* L.)**  
 219 **cultivars. European bread wheat parameters reported by CLRTAP (2017) have been included for comparative purposes.**  
 220 **Parameters are highlighted where there are differences between Indian and European cultivars.**

Bread wheat cultivar parameterisation - POD <sub>6</sub> SPEC				
Parameter	Units	Indo-Gangetic Plains		Atlantic, Boreal, Continental bread wheat (CLRTAP, 2017)
		HUW-234	HD-3118	
$g_{max}$	mmol O <sub>3</sub> m <sup>-2</sup> PLA s <sup>-1</sup>	500	521	500
$f_{min}$	fraction	0.13	0.13	0.01
light_a	-	0.011	0.011	0.011
$T_{min}$	°C	12	12	12
$T_{opt}$	°C	26	26	26
$T_{max}$	°C	40	40	40
VPD <sub>max</sub>	kPa	3.2	3.2	1.2
VDP <sub>min</sub>	kPa	4.6	4.6	3.2



$\Sigma VPD_{crit}$	kPa	16	16	8
$PAW_t^*$	%	50	50	50
$f_{O_3}$	POD <sub>0</sub> mmol O <sub>3</sub> m <sup>-2</sup> PLA s <sup>-1</sup>	14	14	14
Leaf dimension	cm	2	2	2
Canopy height	m	1	1	1
$f_{phen\_a}$	fraction	0.3	0.3	0.3
$f_{phen\_e}$	fraction	0.7	0.7	0.7
$f_{phen\_1\_ETS}$	°C day	-616.6	-553	-200
$f_{phen\_2\_ETS}$	°C day	0	0	0
$f_{phen\_3\_ETS}$	°C day	621.5	553	100
$f_{phen\_4\_ETS}$	°C day	182.75	238	525
$f_{phen\_5\_ETS}$	°C day	959	1000	700

\*PAW<sub>t</sub> is the threshold for plant available water (PAW) in mm above which stomatal conductance is at a maximum

The ETS model (see Eq. 7) was calibrated using experimental data for HUW-234 and HD-3118 that provided the timing (as day of year) of key crop development stages (sowing, emergence, flag leaf emergence, fully expanded flag leaf, start of seed setting, start of senescence and harvest) for both cultivars for 3 years (2016 to 2018 inclusive). Corresponding 3-hourly temperature data were used to estimate daily mean temperature from which ETS values could be determined according to Eq. (7).

$$ETS = \sum (T_i - T_b) \quad [7]$$

Where  $T_i$  is the mean daily temperature and  $T_b$  is the base temperature assumed 0°C for wheat. This is equivalent to the method of thermal time accumulation recommended by CLRTAP (2017) and assumes that there is no upper threshold temperature for phenology and that thermal time increases linearly across the entire temperature range.

The ETS components of the  $f_{phen}$  function from flag leaf emergence were estimated by assuming that  $f_{phen1\_ETS}$  and  $f_{phen3\_ETS}$  together were equivalent to thermal time equally divided between the emerging flag leaf and seed setting. This

precaution ensured  $f_{phen}$  was not allowed to decrease too early; that  $f_{phen5\_ETS}$  less  $f_{phen4\_ETS}$  was equivalent to the thermal time at seed setting less the thermal time at flag leaf emergence and that  $f_{phen1\_ETS}$  and  $f_{phen5\_ETS}$  together were equivalent to the thermal time at harvest less the thermal time at flag leaf emergence; these basic assumptions allowed the derivation of  $f_{phen\_ETS}$  parameters 1-5 given in Table 2. Supplement Figure S1 gives an indication of the year-to-year variability in the timing of these key growth stages used to parameterise the  $f_{phen}$  function. This  $f_{phen}$  function is subsequently used to represent the phenological influence on  $g_{max}$  and to define the seasonal accumulation period for POD<sub>Y</sub>SPEC (see also CLRTAP (2017)). Parameterisation of the  $f_{phen\_ETS}$  model shows little difference in phenology between these cultivars, although HUW-234 had a greater range in dates of flag leaf emergence and fully expanded flag leaf. Seed setting and the start of senescence occurred ~3 days earlier in HD-3118 than HUW-234. The Indian cultivar  $f_{phen\_ETS}$  values differ from the European Continental bread wheat values (also shown in Table 2). In part, this is related to the precautionary approach taken in defining the length of the period during which  $f_{phen}$  will equal 1 to ensure we capture the period when O<sub>3</sub> may be taken up by the stomata in the absence of growth stage data more specific to the  $f_{phen\_ETS}$  stages. The resulting  $f_{phen\_ETS}$  parameterization suggests that Indian cultivars take more thermal time to reach mid-anthesis and less thermal time between the start of senescence and harvest than would bread wheat from the European region.

## 2.6 Model runs

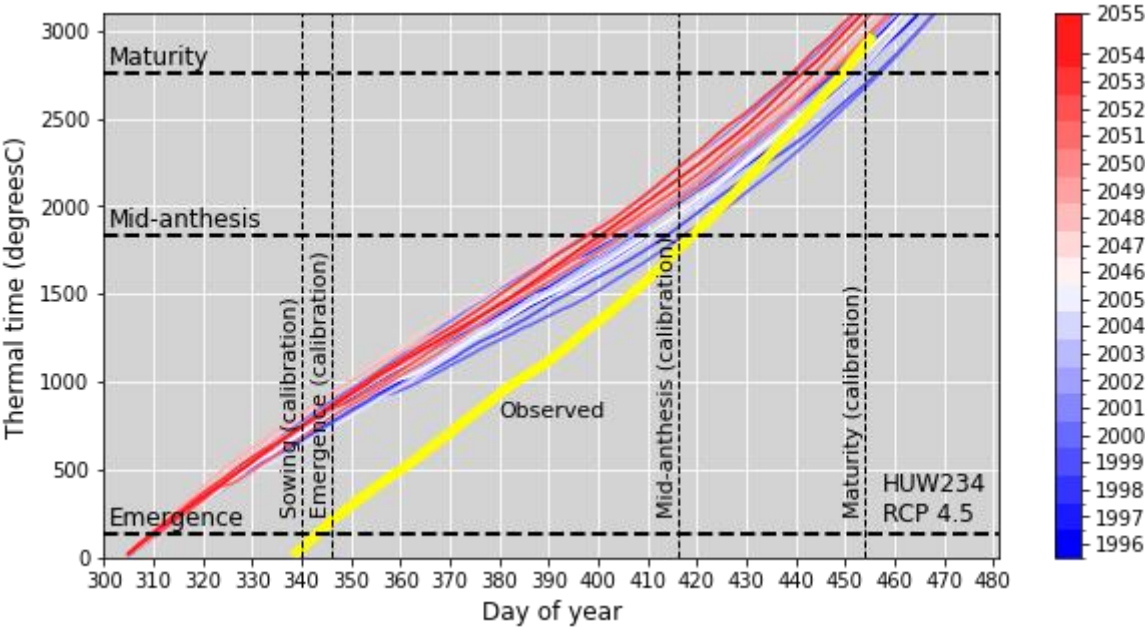
DO<sub>3</sub>SE 3.1.0 model runs were made for each cultivar described in Table 2 using the WRF-Chem modelled O<sub>3</sub> and met data for 1996-2005 which was assumed to represent the recent past climate. The DO<sub>3</sub>SE model runs were repeated for future scenarios using the WRF-Chem modelled O<sub>3</sub> and meteorological data for 2046-2055 based on the two scenarios; RCP4.5 and RCP8.5 to explore the influence of changes in climate and O<sub>3</sub> precursor emissions on O<sub>3</sub> uptake. We assume a sowing date of early November since October to December represent the main sowing months of wheat across the most productive wheat growing states in the IGP (Lobell et al., 2013).

## 3 Results and discussion

### 3.1 Phenology and stomatal O<sub>3</sub> uptake

Accurate modelling of the growing season and the  $f_{phen}$  period in relation to the prevailing O<sub>3</sub> climate is crucial for realistic estimates of O<sub>3</sub> damage to wheat. The ETS model for late-sown cultivars is variable in its ability to simulate key growth stages between years and cultivars. For each growth stage, the minimum and maximum °Cday values between years are 63 to 426°Cday for HUW-234 and 63 to 317°Cday for HD-3118 respectively. Given that the mean daily temperature during the Indian wheat growing season is ~25°C this would suggest the ETS model may have a maximum error of 17 and 13 days for HUW-234 and HD-3118 respectively. These values are likely at the high end of the uncertainty range as temperatures increase during the growing season and the greatest uncertainty was found for the flag leaf emergence and fully expanded

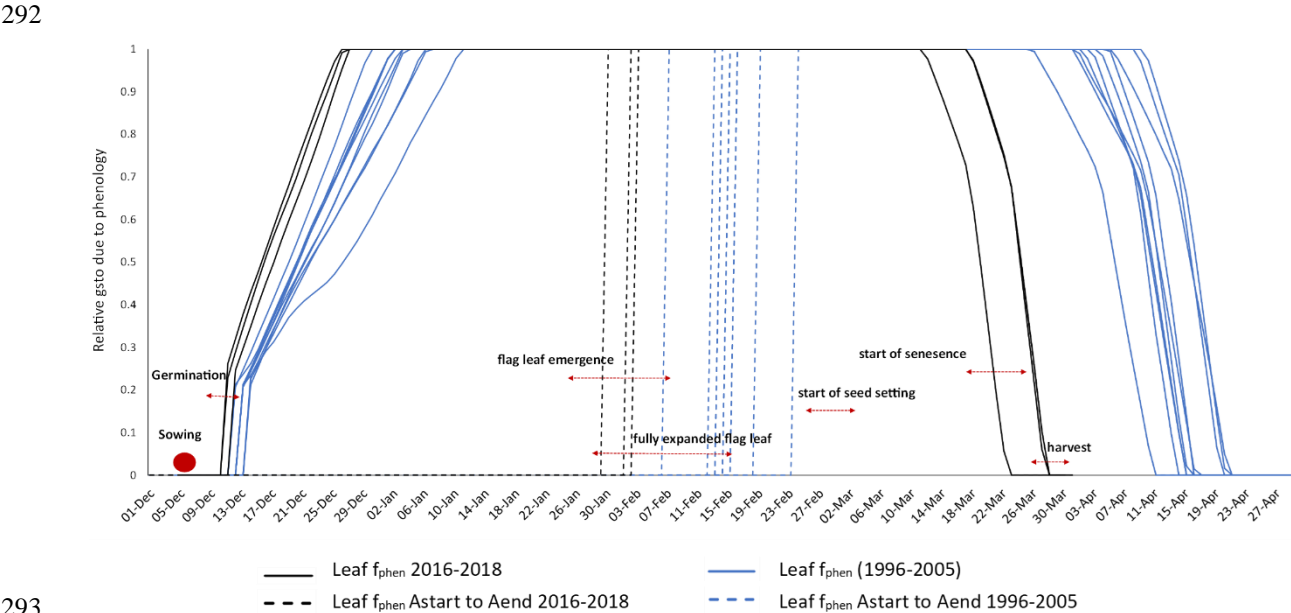
264 flag leaf growth stages. The inclusion of the ‘emerging flag leaf’ in the  $f_{phen}$  period helps to capture the full period when the  
 265 flag leaf may be vulnerable to  $O_3$  as a precaution given the uncertainty in the ETS model defining the timing of the period  
 266 from full flag leaf expansion and senescence.



267  
 268 **Fig. 1: The evolution of ETS and associated growth stages for the observed (2016-18) climate (to which the ETS model is calibrated**  
 269 **with a sowing date of 5<sup>th</sup> Dec) and the WFR-Chem modelled recent past (1986-2005) and future (2046-2055; RCP4.5 and 8.0)**  
 270 **climates (for which the model is applied with a sowing date of 5<sup>th</sup> Nov) for the HUW-234 cultivar.**

271 When the parameterisation was applied to the WRF-Chem modelled 1996-2005 climate temperature data, with a sowing date  
 272 of 5<sup>th</sup> November, maturity is simulated to occur around the end of March (consistent with our observed maturity date of the  
 273 late sown variety under the relatively high temperatures for years 2016-2018 used for parameterisation) – see Fig. 1. Thus  
 274 our  $f_{phen}$  parameterisation, when using standard, early November, sowing dates gives realistic maturity dates for IGP grown  
 275 wheat when used with recent past WRF-Chem modelled data (Fig. 2). Since the WRF-Chem data are consistent between  
 276 climate periods (i.e., 1996-2005 and 2046-2055) they can be deemed to provide a means of comparing the relative effect of  
 277 changes in temperature on the growing season,  $O_3$  uptake and the evolution of soil moisture deficit.  
 278 The empirical data used for model parameterisation collected in years 2016-18, consistently produced higher temperatures  
 279 than the WRF-Chem model-based meteorological data, which was collected from 1996-2005 (Fig. 3a). This could be in part  
 280 due to climate change; average air temperatures in India for 2016, 2017 and 2018 were in the top ten on record since 1901  
 281 (ESSO, 2019). However, on average, 2016-18 was only +0.72°C, +0.55°C and +0.41°C warmer than the 1981-2010 annual  
 282 air temperature average respectively (Earth System Science Organisation et al., 2019), therefore it is likely that uncertainties  
 283 in the modelled values caused the greater part of these discrepancies in temperatures. Since the WRF-Chem model at this  
 284 resolution may not consider some urban heat island effects, a finer model resolution may have led to better agreement with

285 observations for this urban site. Despite this, the nature of the ETS model is that it can provide comparative estimates of the  
 286 influence of temperature profiles on the timing and length of the growing season. Fig 3b shows a similar comparison  
 287 between WRFChem modelled O<sub>3</sub> concentrations (provided as 5 year mean hourly values with absolute minimum and  
 288 maximum bounds also shown) and the ambient air (AA) O<sub>3</sub> concentration data for the 2016-2017 wheat growing season of  
 289 the O<sub>3</sub> experiment. This shows that the WRFChem modelled past climate (1996-2005) data is within range, but at the lower  
 290 end, of the 2016-17 O<sub>3</sub> experimental data as would be expected given the increase in O<sub>3</sub> precursor emissions over the past  
 291 few decades.

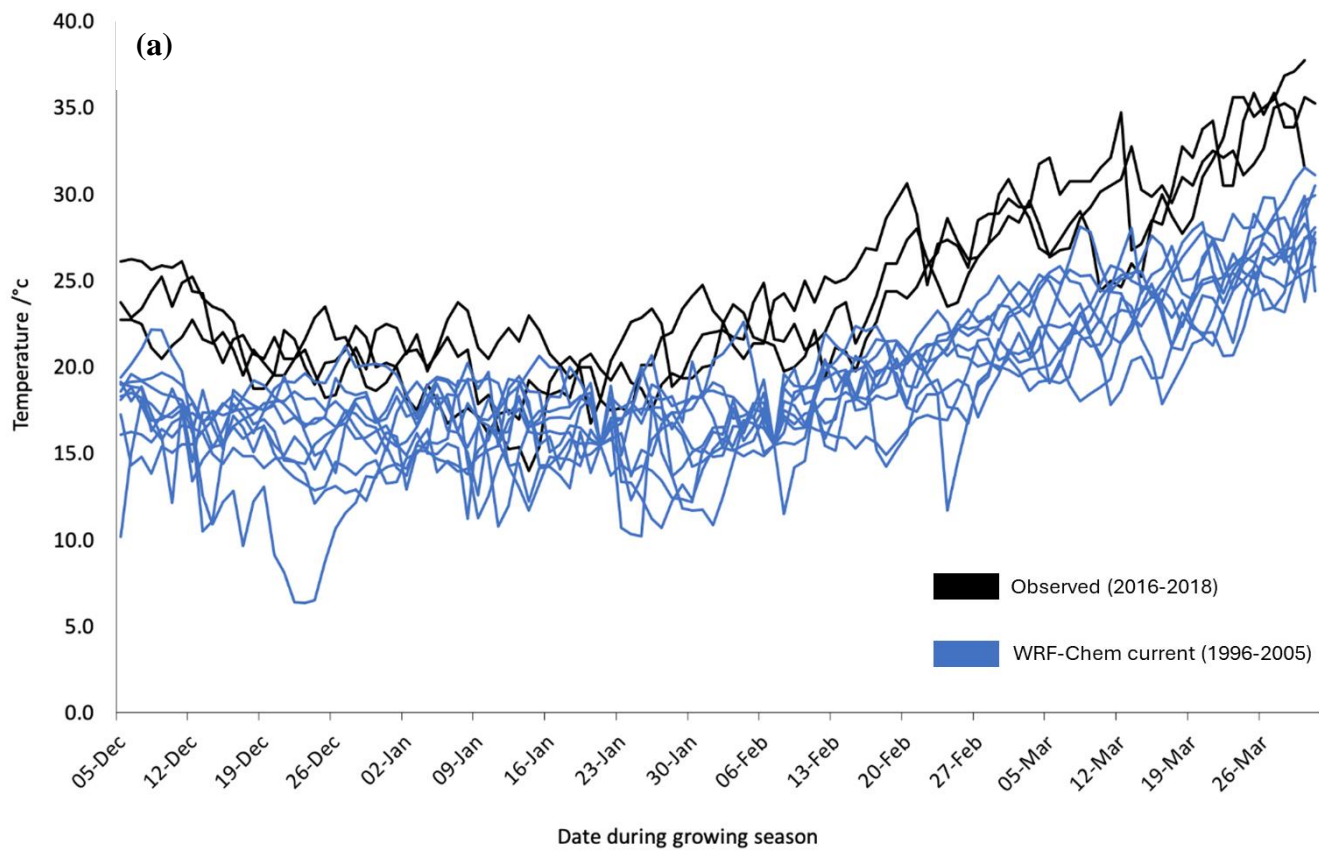


293  
 294 **Fig. 2: The ETS model parameterised for HUW-234 based on observed recent past temperatures (2016-2018; black). The ETS**  
 295 **model for the modelled recent past temperatures (years 1996-2005) are in blue. The range of observed dates of sowing,**  
 296 **germination, flag leaf emergence, fully expanded flag leaf, start of seed setting, start of senescence and harvest from the**  
 297 **experimental data (Agrawal, pers. comm.) are marked with arrows. Astart to Aend represent the start of anthesis to the end of**  
 298 **anthesis.**

307

308

309



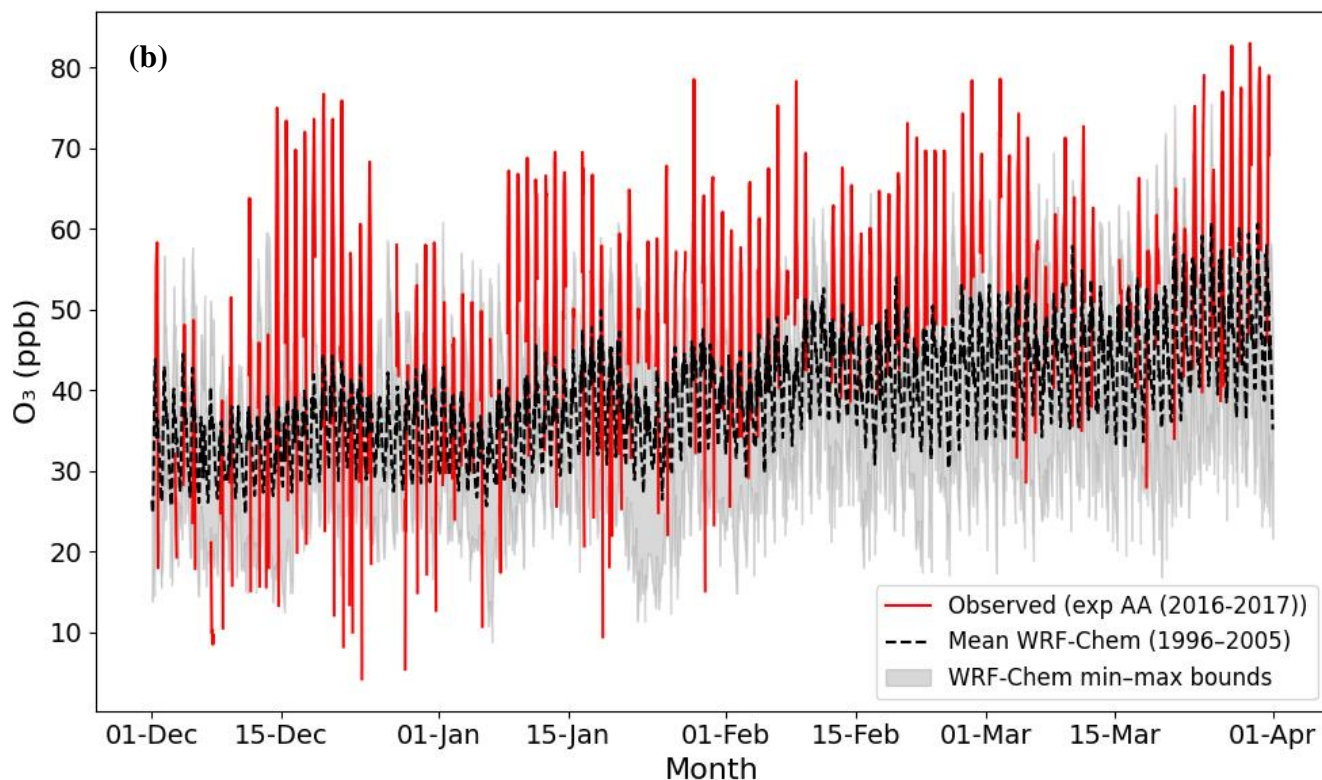


**Fig. 3: Seasonal profiles of (a) surface temperatures over the growing season for observed data (2016-18) and WRF-Chem modelled data for the recent past climate (1996-2005) and (b) O<sub>3</sub> concentration over the growing season for observed data (exp AA (experiment ambient air) for Dec 2016 to Mar 2017 and 10 year (1996 - 2005) annual mean WRF Chem modelled O<sub>3</sub> concentration data with associated absolute minimum and maximum O<sub>3</sub> concentrations bounds also shown.**

The DO<sub>3</sub>SE wheat stomatal O<sub>3</sub> flux model has been evaluated against wheat  $g_{sto}$  data (the primary determinant of stomatal ozone flux) collected under experimental conditions in Ostad, Sweden (Pleijel et al. 2007) and found to perform well (with an R<sup>2</sup> value of 0.83 for a regression of observed against modelled  $g_{sto}$ ). The DO<sub>3</sub>SE model has also been extensively evaluated for a number of crops at locations around the world (as reported in Tuovinen et al. (2004) for wheat growing near Cumono novo in Italy and Emmerichs et al. (2025) for wheat growing near Grignon in France). These evaluations rely on total O<sub>3</sub> flux and deposition measurements (since they use O<sub>3</sub> flux tower data) or water vapour flux measurements and thereby test whole canopy fluxes rather than the representative upper leaf stomatal flux required for PODy calculations. However, the combination of these evaluation methods focussing on both leaf level  $g_{sto}$  and canopy level O<sub>3</sub> flux together provide confidence in the predictive abilities of the DO<sub>3</sub>SE model.

### 3.2 Effect of O<sub>3</sub> stress on the yield benefits of irrigation

Water-stress induced yield loss under rainfed conditions modelled under the climate scenario for 1996-2005 was found to exceed O<sub>3</sub>-relative yield loss (O<sub>3</sub>-RYL) under irrigated conditions for the majority of the 10 years investigated. Under this climate, rainfed conditions produced a mean water-stress relative yield loss (WS-RYL) of 13.3% for HUW-234, with a

330 range of 2.8-31.3% (Fig. 4a). Under rainfed conditions, mean O<sub>3</sub>-RYL was projected to be negligible (0.6%), significantly  
331 lower than the mean O<sub>3</sub>-RYL when no water-stress is assumed under irrigation (10.7% with a range of 4.8-15.4%). This  
332 demonstrates the importance of irrigation for wheat production in India and highlights the substantial influence on the yield of  
333 O<sub>3</sub> for irrigated wheat.

334 O<sub>3</sub>-RYL under irrigated conditions exceeded WS-RYL in 80% of the 10 years investigated in the RCP4.5 scenario (Fig. 4b).  
335 This highlights how O<sub>3</sub> stress negates some of the increased productivity that arises from reducing water stress through  
336 irrigation. In the RCP8.5 scenario, WS-RYL under rainfed conditions exceeded O<sub>3</sub>-RYL under irrigated conditions in all but  
337 one year (2051), when precipitation totaled 234.0mm for the growing season (Fig. 4c). In this scenario, precipitation during  
338 the growing season ranges from 0.9-234.0mm, with a mean of 94±82.97mm, and as a result the WS-RYL fluctuates within the  
339 10 years.

340 Whilst irrigation has played an important role in increasing yields for India's wheat, these results show that O<sub>3</sub> is likely to  
341 negate some of the yield benefits of irrigation. Based on the results of simulations of future climates, irrigation will have less  
342 of an effect on yield increases as [O<sub>3</sub>] levels rise.



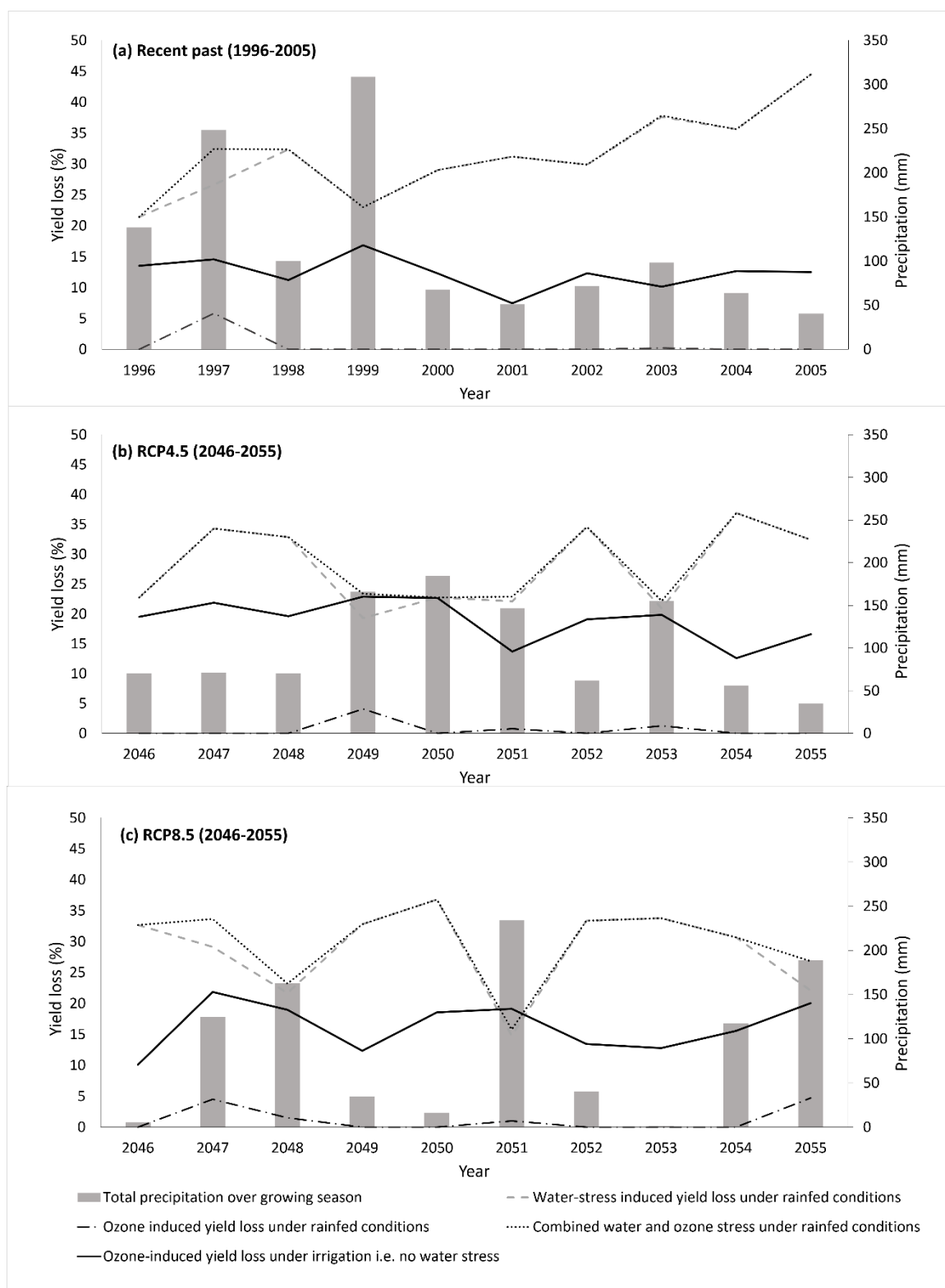


**Fig. 4: The water-stress and ozone-related relative yield loss modelled for HUW-234 under rainfed conditions (water stress) and with no water stress ( $f_{sw}$  set to 1 in DO<sub>3</sub>SE) for (a) the recent past climate 1996-2005; (b) RCP4.5 scenario 2046-2055; (c) RCP8.5 scenario 2046-2055.**

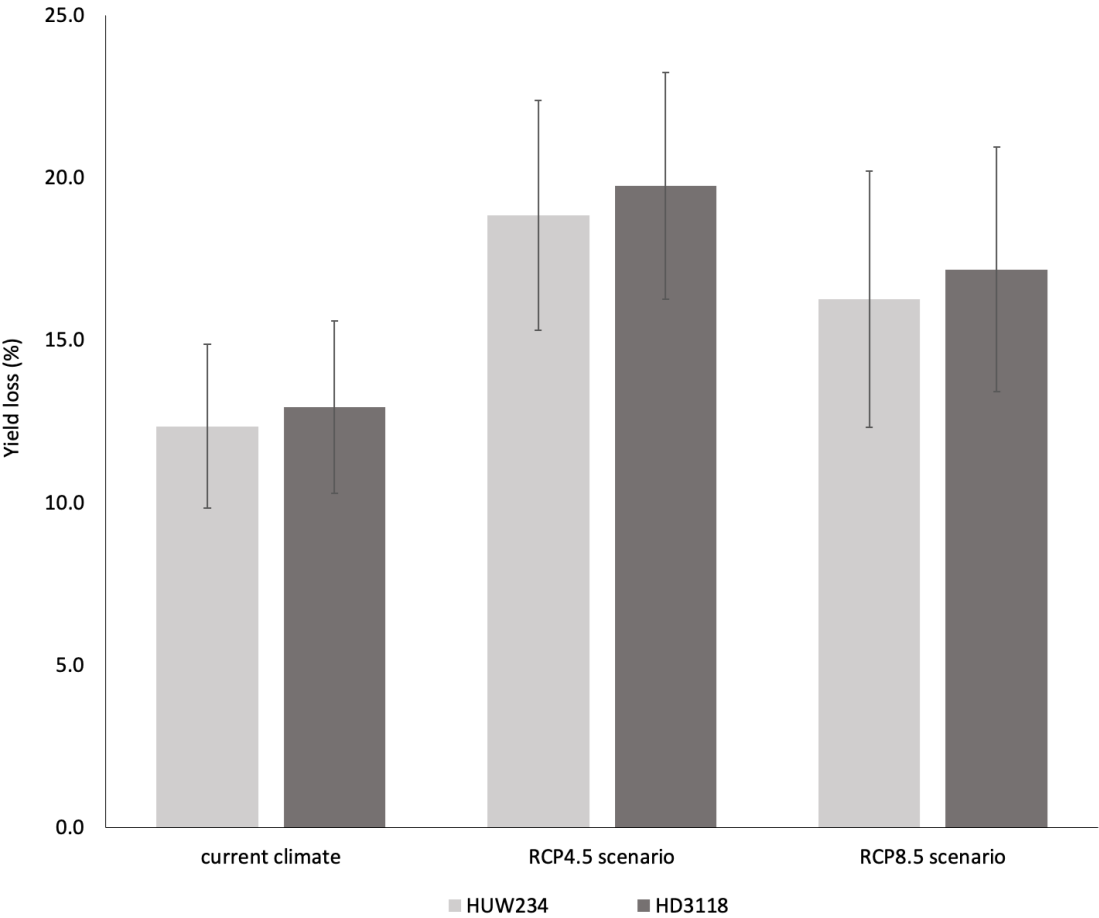
The mean total precipitation for the growing season under the 1996-2005 climate scenario was higher than the median values in the RCP4.5 and RCP8.5 scenarios for 2046-2055, meaning Uttar Pradesh's crops will receive less rainfall in the future. In addition, the RCP8.5 scenario had a larger interquartile range (IQR) of 131.0mm than the 1996-2005 climate (54.8mm) and the smallest lower quartile (22.3mm), demonstrating less and more irregular precipitation in the future climate. Whilst RCP4.5 was less extreme; it had a larger IQR of 90.1mm. This irregularity and increased risk of low precipitation over the growing season demonstrates the continuing importance of irrigation for wheat productivity. In all modelled climate scenarios, water stress tends to be a much greater threat to crop yields than O<sub>3</sub> and therefore, some level of irrigation is crucial for sustained wheat productivity in India. However, these findings clearly show that O<sub>3</sub> is a limiting factor to yield under irrigated conditions meaning that the full potential benefit of irrigation is not being realised and hence will lead to inefficiencies in the use of irrigation water. Further research should be carried out to find the 'sweet spot' for irrigation, that will minimise O<sub>3</sub> stress without inducing water stress, to practice more responsible water management.

Future studies should investigate how short, sharp high O<sub>3</sub> periods could be mitigated with temporary reductions in irrigation, if the efficacy of such approaches can be demonstrated they could be practically applied in the future with the advent of new technologies such as accurate pollution forecasting via machine learning models (Jumin et al., 2020; Wang et al., 2020). A holistic approach that considers the trade-offs between other abiotic stressors such as heat stress is needed, as irrigation plays a significant role in mitigating such stress (Zaveri and Lobell, 2019) and higher temperatures are a precursor of higher O<sub>3</sub> levels with the chance that O<sub>3</sub> effects are erroneously attributed to heat stress (Tai et al., 2014).

### 3.3 Effect of climate change on O<sub>3</sub> sensitivity

Higher O<sub>3</sub>-induced yield losses were modelled under future scenarios (Fig. 5). For HUW234, a statistically significant increase in yield loss of  $7.9 \pm 5.56\%$  and  $3.1 \pm 5.08\%$  was modelled for RCP4.5 and RCP8.5 respectively, compared to the recent past climate. Similarly, for RCP4.5 and RCP8.5, an increase of  $8.0 \pm 5.71\%$  and  $3.0 \pm 4.87\%$  yield loss was predicted for HD-3118, respectively. This suggests that the increase in O<sub>3</sub> impact due to future emissions/climate is larger than the year-to-year variability in O<sub>3</sub> impact for the RCP4.5 (but not RCP8.5 where [O<sub>3</sub>] were lower, see below) scenario. The recent past climate represents the lowest mean O<sub>3</sub>, suggesting O<sub>3</sub>, rather than other environmental conditions that might influence sensitivity to O<sub>3</sub>, (i.e. via alterations to stomatal O<sub>3</sub> uptake) is the most important factor in determining O<sub>3</sub>-induced yield loss. These findings imply that the changing climate (i.e., higher frequency of temperatures that exceed the T<sub>opt</sub> with consequent reductions in stomatal conductance and hence O<sub>3</sub> flux) will be insufficient at ameliorating the increase in O<sub>3</sub>-induced yield loss. This contrasts with several studies that have shown the potential of elevated temperatures to lead to reductions in O<sub>3</sub> flux via reduced stomatal conductance, thus reducing O<sub>3</sub> damage (Emberson et al., 2018; Feng et al., 2008). This could be due to differences in the timing and duration of periods of more extreme temperatures that exist between studies; a possibility that would benefit

377 from further study. It is important to clarify that in this study we explore future changes in ozone concentration due to changes  
 378 in climate due to changes in O<sub>3</sub> precursor emissions. O<sub>3</sub> studies often explore the effect of a ‘climate change penalty’ which is  
 379 the impact of a future climate on O<sub>3</sub> levels if emissions are held constant (Wu et al., 2008; Zanis et al., 2022). Although this is  
 380 not specifically investigated in this study it is worth noting that India is one of the global regions with the strongest effect of a  
 381 ‘climate change penalty’ (Zanis et al 2022). Given the interplay between climate and O<sub>3</sub> in determining the extent of stomatal  
 382 O<sub>3</sub> uptake, and hence crop sensitivity to O<sub>3</sub>, it is worth noting that even without changes in emissions, O<sub>3</sub>-induced crop damage  
 383 would still be likely to change to some extent under future conditions.



384 **Fig. 5: Mean O<sub>3</sub>-induced relative yield losses (O<sub>3</sub>-RYL) ±SD modelled for the recent past climate (1996-2005), and two future**  
 385 **climate scenarios for 2046-2055; RCP4.5 and RCP8.5 for two Indian spring wheat cultivars; HUW-234 and HD-3118.**  
 386

387 The results from this study are within the range published by Mills et al. (2018b) for O<sub>3</sub>-induced yield losses for wheat in Uttar  
 388 Pradesh, which were modelled for 2010-2012 using POD<sub>3</sub>IAM with European wheat parameterisation and a broadscale  
 389 assessment of India’s wheat growing season. The Mills et al. (2018b) study used the most recent methodology from CLRTAP

(2017) to calculate O<sub>3</sub>-induced yield loss for wheat, as a reference POD<sub>3</sub>IAM value representing O<sub>3</sub> uptake at pre-industrial conditions was subtracted before crop loss was calculated. Whilst this study also uses a stomatal flux-based metric, POD<sub>3</sub>IAM is vegetation-type specific suited for large-scale modelling (CLRTAP, 2017). The POD<sub>6</sub>SPEC was used in this current study since we were able to define a cultivar-specific growth period with some certainty thereby allowing greater confidence in the use of the more biologically relevant metric than POD<sub>3</sub>IAM (CLRTAP, 2017). It is also worth noting that the timing of O<sub>3</sub> and water stress may be important in predicting how plants respond to these stresses since O<sub>3</sub> has been found to damage stomatal functioning causing plants lose the ability to respond to water stress (e.g. Wilkinson et al., 2010). Ideally, O<sub>3</sub> impact models would include mechanisms that simulate O<sub>3</sub>-induced loss in stomatal functioning, however, to our knowledge such modelling mechanisms have not yet been developed or included and would likely require experimental data to identify thresholds at which stomatal functioning is impaired.

Mean relative O<sub>3</sub> induced yield losses for both cultivars modelled under RCP4.5 ( $18.7 \pm 3.83\%$ ) were significantly higher than the RCP8.5 ( $13.8 \pm 3.22\%$ ). This is likely due to a combination of slightly higher [O<sub>3</sub>] in RCP4.5 (Table 1) and the WRF-Chem model projections of higher temperatures (limiting O<sub>3</sub> flux as temperatures have a tendency to exceed T<sub>opt</sub>) under RCP8.5. Whilst the RCP4.5 scenario sees a global reduction in [O<sub>3</sub>] due to pollution regulation, the South Asian region is an exception to this rule, where [O<sub>3</sub>] continues to increase at a similar rate as occurred in previous decades (Tai and Martin, 2017). RCP8.5 projects a worldwide increase in [O<sub>3</sub>] due to the lack of regulation of precursor emissions except in parts of the US, East and Southeast Asia (Tai and Martin, 2017). Therefore, mean [O<sub>3</sub>] during the growing season is lowest in the recent past climate at 48.6ppb but similar, at least in South Asia, in both the RCP4.5 and RCP8.5 scenarios (60.5ppb and 59.7ppb respectively; Table 1).

Relatively small differences in 2000-to-2050 increases in O<sub>3</sub> over South Asia between RCP4.5 and RCP8.5 have also been found before (Tai et al., 2014; their Supplementary Figure 1). Our WRF-Chem model results do show a slightly higher increase in O<sub>3</sub> precursors over India in RCP4.5 than RCP8.5 (not shown), likely explaining the slightly higher O<sub>3</sub> increase in the RCP4.5 scenario. However, several factors influence the modelled future O<sub>3</sub> concentration changes, such as the future change in meteorological variables, the non-linearities of O<sub>3</sub> chemistry, and natural interannual variability. For example, Sharma et al. (2023) found underestimation of relative humidity in meteorological data used in O<sub>3</sub> simulations which will have some influence on O<sub>3</sub> production estimates. Future studies should utilize emission scenarios that are more updated in terms of air pollution policies.

The O<sub>3</sub>-induced yield loss will increase from current levels, regardless of whether global emissions follow a business-as-usual or medium stabilisation scenario. We predict that O<sub>3</sub>-induced yield losses will continue to increase in South Asia with climate change, given the co-emission of radiative forcers and O<sub>3</sub> precursors and the two-way causality that exists between O<sub>3</sub> formation and climate change, i.e., hot, sunny conditions likely to be enhanced under climate change encourages O<sub>3</sub> formation, whilst O<sub>3</sub> itself is a radiative forcer (Fu and Tian, 2019). This means that O<sub>3</sub> and climate variable stress are likely to co-occur in the future which becomes especially problematic for crop productivity when environmental thresholds (e.g. due to temperature extremes) for plant productivity are exceeded. South Asia and the IGP are important agricultural regions where

O<sub>3</sub> thresholds are being exceeded now (Mills et al., 2018c), with the likelihood that the extent of such exceedance will only worsen in the future and with climate change (Cooper et al., 2014; Fowler et al., 2008; Fu and Tian, 2019; Rathore et al., 2023). It should be noted that there are uncertainties in the WRF-Chem model used in modelling meteorological and [O<sub>3</sub>] data. There are important criticisms that the WRF-Chem model is limited in its ability in capturing true wind speeds, which influences temperature and O<sub>3</sub> mixing ratios (Rydsaa et al., 2016). Despite this, these findings serve as a useful insight into the future risk of O<sub>3</sub> on wheat yields relative to early 21<sup>st</sup>-century conditions. Ideally, future research should consider the use of model ensembles to more robustly capture ranges in future meteorological and [O<sub>3</sub>] data.

### 3.4 Influence of cultivar physiology on O<sub>3</sub> sensitivity

The O<sub>3</sub>-RYL modelled for HUW-234 were similar to HD-3118 in the recent past climate and both the RCP4.5 and RCP8.5 scenarios (Fig. 5). This is due to the similarity in  $g_{max}$  values for HUW-234 and HD-3118 which were estimated, from empirical data at 500mmol O<sub>3</sub> m<sup>-2</sup> PLA s<sup>-1</sup> and 520.9 mmol O<sub>3</sub> m<sup>-2</sup> PLA s<sup>-1</sup> respectively. The mean yield losses for recent past climate and RCP scenarios combined, modelled for HD-3118 (14.5±0.05%) were similar to HUW-234 (14.3±0.05%), a difference of 0.2%. Despite the similar mean yield losses observed for HD-3118 and HUW-234, these results align with concerns that modern wheat cultivars are more susceptible to O<sub>3</sub>-damage as they are bred for maximum gas exchange or heat tolerance rather than O<sub>3</sub> tolerance (Emberson et al., 2018; Pleijel et al., 2006; Yadav et al., 2020). Typically, plant traits bred for heat tolerance and maximum gas exchange conflict with traits for O<sub>3</sub> tolerance and may increase irrigation requirements; i.e. higher stomatal conductance enhances transpiration rates, allowing for higher rates of photosynthesis (Pleijel et al., 2007; Yadav et al., 2020). Despite the potential for HD-3118 to produce higher yields due to a high stomatal conductance, HUW-234 performs better in terms of O<sub>3</sub> tolerance for Varanasi's recent past conditions and projections for the future climate and [O<sub>3</sub>]. This is also observed in the empirical data for Varanasi from 2016-18, which was used to parameterise the ETS model. The empirical data observed lower relative yield loss under elevated [O<sub>3</sub>] compared to ambient [O<sub>3</sub>] for HUW-234 than HD-3118 (21.2% and 23.2% respectively; see Table S1). Absolute yields failed to observe the higher yielding potential expected of HD-3118 even under ambient conditions; the mean absolute grain yield for HUW-234 under ambient [O<sub>3</sub>] was 533.4g/m compared to 432.8g/m for HD-3118. Under elevated [O<sub>3</sub>], the yield gap widens; HUW-234 has an absolute grain yield of 420.4g/m whilst HD-3118 has a yield of 332.3g/m. This suggests O<sub>3</sub> has a greater impact on yield in HD-3118 than HUW-234, possibly even under ambient concentrations.

Despite corroborating literature for the DO<sub>3</sub>SE model results (Yadav et al., 2020), there is some limitation in the ability to accurately parameterise the model for specific cultivars. Here we have been able to parameterise key parameters that will influence stomatal O<sub>3</sub> flux ( $g_{max}$  and  $f_{phen}$ ) for Indian varieties, however, the remaining parameters that determine the modification of  $g_{max}$  by environmental conditions rely on European parameterisations. Similarly, the DO<sub>3</sub>SE model estimates O<sub>3</sub>-induced crop yield losses based on a dose-response relationship configured using five European wheat cultivars (CLRTAP, 2017). Whilst the DO<sub>3</sub>SE model is a valuable tool for risk assessment, the use of appropriately calibrated and evaluated crop models will provide mechanisms to fully explore the interplay between stresses such as O<sub>3</sub> and water stress on yield (Emberson

et al., 2018). The results of this paper make clear the need for such modelling to improve our understanding of how these different stresses act over the course of the growing season to determine changes in productivity. A new generation of crop models that are being developed to incorporate the O<sub>3</sub> effect, as well as other stresses (Emberson et al., 2018), will be able to explore trade-offs between stresses related to soil water, extreme temperatures, and soil fertility. Such advances in crop modelling will be crucial in assessing future wheat productivity under a range of abiotic stress conditions.

In this Indian study, the mid-anthesis and grain filling period occurred in March (Fig.'s 1 and 2) which corresponds to peak O<sub>3</sub> in Uttar Pradesh (Jain et al., 2023; Mukherjee et al., 2019; Shukla et al., 2017). However, a study on timely-sown Chinese winter wheat cultivars found that elevated O<sub>3</sub> only had a significant effect during the mid-grain filling stage, suggesting that timing mid-grain filling with O<sub>3</sub> troughs could be a mitigation strategy, which may be achieved by earlier sowing (Feng et al., 2016). Late planting results in reduced productivity of the wheat crop, with earlier, timely sowing of wheat in the third week of November yielding the best productivity in Eastern Uttar Pradesh (Chandna et al., 2004). Past studies have reported that delays in sowing after mid-November leads to reduction in yield of wheat, often at a rate of 1-1.5% per day (McDonald et al., 2022; Ortiz-Monasterio R. et al., 1994). In addition, Kumar et al. (2014) claimed conversion from late to timely-sown would offset the impacts of climate change. A multi-tolerance approach like early sowing could mitigate heat and O<sub>3</sub> stress however, late sowing is often due to delays in harvesting rice in Rice-Wheat systems, a cropping sequence which provides income for tens of millions of farm families (Jain et al., 2017; Mishra et al., 2021). Further investigation of the inter-play between [O<sub>3</sub>] profiles over the growing season and targeted crop phenology of different cultivar types should be conducted.

#### 4 Conclusion

Whilst irrigation has played a pivotal role in increasing wheat production in India through maximising yields, O<sub>3</sub> is likely to negate some of the yield benefits of irrigation, which will reduce irrigation efficiency. Based on the POD<sub>6</sub>SPEC values obtained *via* the DO<sub>3</sub>SE model and associated flux-response relationships, O<sub>3</sub> concentrations prevalent in the IGP region of India are high enough to cause grain yield losses in Indian wheat. This paper demonstrates the complexity of avoiding O<sub>3</sub>-stress and the importance of taking a multi-stress approach to mitigation. Since high levels of O<sub>3</sub> typically coincide with other abiotic stressors such as heat stress, the approach taken to maximise crop yield must consider multiple stressors and their interactions. Rather than altering irrigation patterns to mitigate O<sub>3</sub> stress and risk increasing the effect of other stressors such as water stress or heat stress, earlier sowing to avoid peak O<sub>3</sub> and temperatures in March may benefit irrigated wheat growing in India. Given that modern wheat cultivars are more O<sub>3</sub>-sensitive, wheat growers should reconsider using modern cultivars bred for optimal gas exchange.

#### Competing interests

The contact author has declared that none of the authors has any competing interests

## Author Contribution

GE and LE designed the modelling study and GE and SB performed the DO<sub>3</sub>SE model runs. OH provided the modelled O<sub>3</sub> and meteorological data and advised on its use within the study. MA and DSY provided the experimental data used to calibrate the DO<sub>3</sub>SE model and advised on its use within the study. CON, CJ, JC and PP supported DO<sub>3</sub>SE model calibration and analysis of the results. GE prepared the manuscript with contributions from all co-authors.

## Acknowledgements

Funding from The Norwegian Research Council funded CICERO strategic project (grant no. 160015/F40) and the CiXPAG project (grant no. 244551) provided support to Lisa Emberson, Øivind Hodnebrog and Madhoolika Agrawal. The Viking cluster was used during this project, which is a high-performance computing facility provided by the University of York. We are grateful for computational support from the University of York, IT Services and the Research IT team.

## References

- Ainsworth, E. A., Rogers, A., and Leakey, A. D. B.: Targets for crop biotechnology in a future high-CO<sub>2</sub> and high-O<sub>3</sub> world, *Plant Physiol.*, 147, 13–19, <https://doi.org/10.1104/pp.108.117101>, 2008.
- Ali, M., Jensen, C. R., Mogensen, V. O., Andersen, M. N., and Henson, I. E.: Root signalling and osmotic adjustment during intermittent soil drying sustain grain yield of field grown wheat, *F. Crop. Res.*, 62, 35–52, [https://doi.org/10.1016/S0378-4290\(99\)00003-9](https://doi.org/10.1016/S0378-4290(99)00003-9), 1999.
- Amnuaylojaroen, T., Macatangay, R. C., Khodmanee, S.: Modeling the effect of VOCs from biomass burning emissions on ozone pollution in upper Southeast Asia. *Heliyon*. 2019 Oct 17, 5(10):e02661, <https://doi.org/10.1016/j.heliyon.2019.e02661>.
- Broberg, M. C., Hayes, F., Harmens, H., Uddling, J., Mills, G., and Pleijel, H.: Effects of ozone, drought and heat stress on wheat yield and grain quality, *Agric. Ecosyst. Environ.*, 352, <https://doi.org/10.1016/j.agee.2023.108505>, 2023.
- Büker, P., Morrissey, T., Briolat, A., Falk, R., Simpson, D., Tuovinen, J. P., Alonso, R., Barth, S., Baumgarten, M., Grulke, N., Karlsson, P. E., King, J., Lagergren, F., Matyssek, R., Nunn, A., Ogaya, R., Pêuelas, J., Rhea, L., Schaub, M., Uddling, J., Werner, W., and Emberson, L. D.: DO<sub>3</sub>SE modelling of soil moisture to determine ozone flux to forest trees, *Atmos. Chem. Phys.*, 12, 5537–5562, <https://doi.org/10.5194/acp-12-5537-2012>, 2012.
- Chandna, P., Hodson, D. P., Singh, U. P., Singh, A. N., Gosain, A. K., Sahoo, R. N., and Gupta, R. K.: Increasing the Productivity of Underutilized Lands by Targeting Resource Conserving Technologies-A GIS/Remote Sensing Approach: A Case Study of Ballia District, Uttar Pradesh, in the Eastern Gangentic Plains, 43 pp., 2004.
- CLRTAP: Chapter 3: Mapping critical levels for vegetation, in: Manual on methodologies and criteria for modelling and mapping critical loads and levels and air pollution effects, risks and trends, 2017.

519 Conway, T.J., n.d.. Global mean growth rates. [online] viewed 8 February 2020, available at:  
 520 <https://data.giss.nasa.gov/modelforce/ghgases/Fig1A.ext.txt>.

521 Cooper, O. R., Parrish, D. D., Ziemke, J., Balashov, N. V., Cupeiro, M., Galbally, I. E., Gilge, S., Horowitz, L., Jensen, N. R.,  
 522 Lamarque, J. F., Naik, V., Oltmans, S. J., Schwab, J., Shindell, D. T., Thompson, A. M., Thouret, V., Wang, Y., and Zbinden,  
 523 R. M.: Tropospheric Ozone Assessment Report: Global distribution and trends of tropospheric ozone: An observation-based  
 524 review, *Elem. Sci. Anthr.*, 2, 1–28, <https://doi.org/10.12952/journal.elementa.000029>, 2014.

525 Daloz, A. S., Rydsaa, J. H., Hodnebrog, Sillmann, J., van Oort, B., Mohr, C. W., Agrawal, M., Emberson, L., Stordal, F., and  
 526 Zhang, T.: Direct and indirect impacts of climate change on wheat yield in the Indo-Gangetic plain in India, *J. Agric. Food*  
 527 *Res.*, 4, 100132, <https://doi.org/10.1016/j.jafr.2021.100132>, 2021.

528 Doorenbos, J. and Kassam, A. H.: Crop yield response to water, FAO Irrig. Drain. Pap. no. 33, 33, 1979.

529 Earth System Science Organisation, Ministry of Earth Sciences, Indian Meteorological Department, and Climate Research and  
 530 Services: Statement on climate of India during 2018, 2019.

531 Emberson, L. D., Ashmore, M. R., Cambridge, H. M., Simpson, D., and Tuovinen, J. : Modelling stomatal ozone flux across  
 532 Europe, *Environ. Pollut.*, 109, 403–413, 2000a.

533 Emberson, L. D., Simpson, D., Tuovinen, J., Ashmore, M. R., and Cambridge, H. M.: Towards a model of ozone deposition  
 534 and stomatal uptake over Europe, in: Research Note No. 42, EMEP/MSC-W 6/2000, 2000b.

535 Emberson, L. D., Pleijel, H., Ainsworth, E. A., van den Berg, M., Ren, W., Osborne, S., Mills, G., Pandey, D., Dentener, F.,  
 536 Büker, P., Ewert, F., Koeble, R., and Van Dingenen, R.: Ozone effects on crops and consideration in crop models, *Eur. J.*  
 537 *Agron.*, 100, 19–34, <https://doi.org/10.1016/j.eja.2018.06.002>, 2018.

538 Emmerichs, T., Al Mamun, A., Emberson, L., Mao, H., Zhang, L., Ran, L., Betancourt, C., Wong, A., Koren, G., Gerosa, G.,  
 539 Huang, M., and Guaita, P.: Can atmospheric chemistry deposition schemes reliably simulate stomatal ozone flux across global  
 540 land covers and climates?, *EGUsphere* [preprint], <https://doi.org/10.5194/egusphere-2025-429>, 2025.

541 Fangmeier, A., Brockerhoff, U., Grüters, U., and Jäger, H. J.: Growth and yield responses of spring wheat (*Triticum aestivum*  
 542 L. CV. Turbo) grown in open-top chambers to ozone and water stress, *Environ. Pollut.*, 83, 317–325,  
 543 [https://doi.org/10.1016/0269-7491\(94\)90153-8](https://doi.org/10.1016/0269-7491(94)90153-8), 1994.

544 Farooq, M., Hussain, M., and Siddique, K. H. M.: Drought Stress in Wheat during Flowering and Grain-filling Periods, *CRC.*  
 545 *Crit. Rev. Plant Sci.*, 33, 331–349, <https://doi.org/10.1080/07352689.2014.875291>, 2014.

546 Feng, Z., Kobayashi, K., and Ainsworth, E. A.: Impact of elevated ozone concentration on growth, physiology, and yield of  
 547 wheat (*Triticum aestivum* L.): A meta-analysis, *Glob. Chang. Biol.*, 14, 2696–2708, <https://doi.org/10.1111/j.1365-2486.2008.01673.x>, 2008.

549 Feng, Z., Wang, L., Pleijel, H., Zhu, J., and Kobayashi, K.: Differential effects of ozone on photosynthesis of winter wheat  
 550 among cultivars depend on antioxidative enzymes rather than stomatal conductance, *Sci. Total Environ.*, 572, 404–411,  
 551 <https://doi.org/10.1016/j.scitotenv.2016.08.083>, 2016.



552 Fischer, G., Tubiello, F. N., van Velthuizen, H., and Wiberg, D. A.: Climate change impacts on irrigation water requirements:  
 553 Effects of mitigation, 1990-2080, Technol. Forecast. Soc. Change, 74, 1083–1107,  
 554 <https://doi.org/10.1016/j.techfore.2006.05.021>, 2007.

555 Fishman, R.: Groundwater depletion limits the scope for adaptation to increased rainfall variability in India, Clim. Change,  
 556 147, 195–209, <https://doi.org/10.1007/s10584-018-2146-x>, 2018.

557 Fowler, D., Amann, M., Anderson, R., Ashmore, M., Cox, P., Depledge, M., Derwent, D., Grennfelt, P., Hewitt, N., Hov, O.,  
 558 Jenkin, M., Kelly, F., Liss, P., Pilling, M., Pyle, J., Slingo, J., and Stevenson, D.: Ground-level ozone in the 21st century: future  
 559 trends, impacts and policy implications, 134 pp., 2008.

560 Fu, T. M. and Tian, H.: Climate Change Penalty to Ozone Air Quality: Review of Current Understandings and Knowledge  
 561 Gaps, Curr. Pollut. Reports, 5, 159–171, <https://doi.org/10.1007/s40726-019-00115-6>, 2019.

562 Gelang, J., Pleijel, H., Sild, E., Danielsson, H., Younis, S., and Selldén, G.: Rate and duration of grain filling in relation to flag  
 563 leaf senescence and grain yield in spring wheat (*Triticum aestivum*) exposed to different concentrations of ozone, Physiol.  
 564 Plant., 110, 366–375, <https://doi.org/10.1111/j.1399-3054.2000.1100311.x>, 2000.

565 Gent, P. R., Danabasoglu, G., Donner, L. J., Holland, M. M., Hunke, E. C., Jayne, S. R., Lawrence, D. M., Neale, R. B., Rasch,  
 566 P. J., Vertenstein, M., Worley, P. H., Yang, Z. L., and Zhang, M.: The community climate system model version 4, J. Clim.,  
 567 24, 4973–4991, <https://doi.org/10.1175/2011JCLI4083.1>, 2011.

568 Ghosh, A., Agrawal, M., and Agrawal, S. B.: Effect of water deficit stress on an Indian wheat cultivar (*Triticum aestivum* L.  
 569 HD 2967) under ambient and elevated level of ozone, Sci. Total Environ., 714, 136837,  
 570 <https://doi.org/10.1016/j.scitotenv.2020.136837>, 2020.

571 Ghude, S. D., Jena, C., Chate, D. M., Beig, G., Pfister, G. G., Kumar, R., and Ramanathan, V.: Reductions in India’s crop yield  
 572 due to ozone, Geophys. Res. Lett., 41, 5685–5691, <https://doi.org/10.1002/2014GL060930>, 2014.

573 Grell, G. A., Peckham, S. E., Schmitz, R., McKeen, S. A., Frost, G., Skamarock, W. C., and Eder, B.: Fully coupled “online”  
 574 chemistry within the WRF model, Atmos. Environ., 39, 6957–6975, <https://doi.org/10.1016/j.atmosenv.2005.04.027>, 2005.

575 Harmens, H., Hayes, F., Sharps, K., Radbourne, A., and Mills, G.: Can reduced irrigation mitigate ozone impacts on an ozone-  
 576 sensitive african wheat variety?, Plants, 8, <https://doi.org/10.3390/plants8070220>, 2019.

577 Haworth, M., Marino, G., Loreto, F., and Centritto, M.: Integrating stomatal physiology and morphology: evolution of stomatal  
 578 control and development of future crops, Oecologia, 197, 867–883, <https://doi.org/10.1007/s00442-021-04857-3>, 2021.

579 He, C. and Zhou, T.: Responses of the western North Pacific subtropical high to global warming under RCP4.5 and RCP8.5  
 580 scenarios projected by 33 CMIP5 models: The dominance of tropical Indian Ocean-tropical western Pacific SST gradient, J.  
 581 Clim., 28, 365–380, <https://doi.org/10.1175/JCLI-D-13-00494.1>, 2015.

582 Hodnebrog, O., Marelle, L., Alterskjær, K., Wood, R. R., Ludwig, R., Fischer, E. M., Richardson, T. B., Forster, P. M.,  
 583 Sillmann, J., and Myhre, G.: Intensification of summer precipitation with shorter time-scales in Europe, Environ. Res. Lett.,  
 584 14, <https://doi.org/10.1088/1748-9326/ab549c>, 2019.

585 Houshmandfar, A., Fitzgerald, G. J., O’Leary, G., Tausz-Posch, S., Fletcher, A., and Tausz, M.: The relationship between  
586 transpiration and nutrient uptake in wheat changes under elevated atmospheric CO<sub>2</sub>, *Physiol. Plant.*, 163, 516–529,  
587 <https://doi.org/10.1111/ppl.12676>, 2018.

588 Jain, M., Singh, B., Srivastava, A. A. K., Malik, R. K., McDonald, A. J., and Lobell, D. B.: Using satellite data to identify the  
589 causes of and potential solutions for yield gaps in India’s Wheat Belt, *Environ. Res. Lett.*, 12, [https://doi.org/10.1088/1748-](https://doi.org/10.1088/1748-9326/aa8228)  
590 [9326/aa8228](https://doi.org/10.1088/1748-9326/aa8228), 2017.

591 Jain, V., Tripathi, N., Tripathi, S. N., Gupta, M., Sahu, L. K., Murari, V., Gaddamidi, S., Shukla, A. K., and Prevot, A. S. H.:  
592 Real-time measurements of non-methane volatile organic compounds in the central Indo-Gangetic basin, Lucknow, India:  
593 source characterisation and their role in O<sub>3</sub> and secondary organic aerosol formation, *Atmos. Chem. Phys.*, 23, 3383–3408,  
594 <https://doi.org/10.5194/acp-23-3383-2023>, 2023.

595 Joshi, A. K., Chand, R., Arun, B., Singh, R. P., and Ortiz, R.: Breeding crops for reduced-tillage management in the intensive,  
596 rice-wheat systems of South Asia, *Euphytica*, 153, 135–151, <https://doi.org/10.1007/s10681-006-9249-6>, 2007.

597 Jumin, E., Zaini, N., Ahmed, A. N., Abdullah, S., Ismail, M., Sherif, M., Sefelnasr, A., and El-Shafie, A.: Machine learning  
598 versus linear regression modelling approach for accurate ozone concentrations prediction, *Eng. Appl. Comput. Fluid Mech.*,  
599 14, 713–725, <https://doi.org/10.1080/19942060.2020.1758792>, 2020.

600 Kangasjärvi, J., Jaspers, P., and Kollist, H.: Signalling and cell death in ozone-exposed plants, *Plant, Cell Environ.*, 28, 1021–  
601 1036, <https://doi.org/10.1111/j.1365-3040.2005.01325.x>, 2005.

602 Khan, S. and Soja, G.: Yield responses of wheat to zone exposure as modified by drought-induced differences in ozone uptake,  
603 *Water. Air. Soil Pollut.*, 147, 299–315, <https://doi.org/10.1023/A:1024577429129>, 2003.

604 Kumar, S. N., Aggarwal, P. K., Swaroopa Rani, D. N., Saxena, R., Chauhan, N., and Jain, S.: Vulnerability of wheat production  
605 to climate change in India, *Clim. Res.*, 59, 173–187, <https://doi.org/10.3354/cr01212>, 2014.

606 Lamarque, J. F., Bond, T. C., Eyring, V., Granier, C., Heil, A., Klimont, Z., Lee, D., Liousse, C., Mieville, A., Owen, B.,  
607 Schultz, M. G., Shindell, D., Smith, S. J., Stehfest, E., Van Aardenne, J., Cooper, O. R., Kainuma, M., Mahowald, N.,  
608 McConnell, J. R., Naik, V., Riahi, K., and Van Vuuren, D. P.: Historical (1850-2000) gridded anthropogenic and biomass  
609 burning emissions of reactive gases and aerosols: Methodology and application, *Atmos. Chem. Phys.*, 10, 7017–7039,  
610 <https://doi.org/10.5194/acp-10-7017-2010>, 2010.

611 Lamarque, J. F., Kyle, P. P., Meinshausen, M., Riahi, K., Smith, S. J., van Vuuren, D. P., Conley, A. J., and Vitt, F.: Global  
612 and regional evolution of short-lived radiatively-active gases and aerosols in the Representative Concentration Pathways, *Clim.*  
613 *Change*, 109, 191–212, <https://doi.org/10.1007/s10584-011-0155-0>, 2011.

614 Lobell, D. B., Ortiz-Monasterio, J. I., Sibley, A. M., and Sohu, V. S.: Satellite detection of earlier wheat sowing in India and  
615 implications for yield trends, *Agric. Syst.*, 115, 137–143, <https://doi.org/10.1016/j.agsy.2012.09.003>, 2013.

616 McDonald, A. J., Balwinder-Singh, Keil, A., Srivastava, A., Craufurd, P., Kishore, A., Kumar, V., Paudel, G., Singh, S., Singh,  
617 A. K., Sohane, R. K., and Malik, R. K.: Time management governs climate resilience and productivity in the coupled rice–  
618 wheat cropping systems of eastern India, *Nat. Food*, 3, 542–551, <https://doi.org/10.1038/s43016-022-00549-0>, 2022.

Meinshausen, M., Smith, S. J., Calvin, K., Daniel, J. S., Kainuma, M. L. T., Lamarque, J., Matsumoto, K., Montzka, S. A., Raper, S. C. B., Riahi, K., Thomson, A., Velders, G. J. M., and van Vuuren, D. P. P.: The RCP greenhouse gas concentrations and their extensions from 1765 to 2300, *Clim. Change*, 109, 213–241, <https://doi.org/10.1007/s10584-011-0156-z>, 2011.

Mills, G., Sharps, K., Simpson, D., Pleijel, H., Frei, M., Burkey, K., Emberson, L., Uddling, J., Broberg, M., Feng, Z., Kobayashi, K., and Agrawal, M.: Closing the global ozone yield gap: Quantification and cobenefits for multistress tolerance, *Glob. Chang. Biol.*, 24, 4869–4893, <https://doi.org/10.1111/gcb.14381>, 2018a.

Mills, G., Sharps, K., Simpson, D., Pleijel, H., Broberg, M., Uddling, J., Jaramillo, F., Davies, W. J., Dentener, F., Van den Berg, M., Agrawal, M., Agrawal, S. B., Ainsworth, E. A., Büker, P., Emberson, L., Feng, Z., Harmens, H., Hayes, F., Kobayashi, K., Paoletti, E., and Van Dingenen, R.: Ozone pollution will compromise efforts to increase global wheat production, *Glob. Chang. Biol.*, 24, 3560–3574, <https://doi.org/10.1111/gcb.14157>, 2018b.

Mills, G., Pleijel, H., Malley, C. S., Sinha, B., Cooper, O. R., Schultz, M. G., Neufeld, H. S., Simpson, D., Sharps, K., Feng, Z., Gerosa, G., Harmens, H., Kobayashi, K., Saxena, P., Paoletti, E., Sinha, V., and Xu, X.: Tropospheric Ozone Assessment Report: Present-day ozone distribution and trends relevant to human health, *Elem. Sci. Anthr.*, 6, <https://doi.org/10.1525/elementa.302>, 2018.

Ministry of Agriculture & Farmers Welfare: Agricultural Statistics at a Glance 2021, New Delhi, 431 pp., 2022.

Mishra, J. S., Poonia, S. P., Kumar, R., Dubey, R., Kumar, V., Mondal, S., Dwivedi, S. K., Rao, K. K., Kumar, R., Tamta, M., Verma, M., Saurabh, K., Kumar, S., Bhatt, B. P., Malik, R. K., McDonald, A., and Bhaskar, S.: An impact of agronomic practices of sustainable rice-wheat crop intensification on food security, economic adaptability, and environmental mitigation across eastern Indo-Gangetic Plains, *F. Crop. Res.*, 267, 108164, <https://doi.org/10.1016/j.fcr.2021.108164>, 2021.

Montieth, J. L.: Evaporation and environment, *Symp. Soc. Exp. Biol.*, 19, 205–234, 1965.

Morgan, J. M.: Osmoregulation and Water Stress in Higher Plants, *Annu. Rev. Plant Physiol.*, 35, 299–319, <https://doi.org/10.1146/annurev.pp.35.060184.001503>, 1984.

Mukherjee, A., Wang, S. Y. S., and Promchote, P.: Examination of the climate factors that reduced wheat yield in northwest India during the 2000s, *Water*, 11, 1–13, <https://doi.org/10.3390/w11020343>, 2019.

Nigam, R., Vyas, S. S., Bhattacharya, B. K., Oza, M. P., and Manjunath, K. R.: Retrieval of regional LAI over agricultural land from an Indian geostationary satellite and its application for crop yield estimation, *J. Spat. Sci.*, 62, 103–125, <https://doi.org/10.1080/14498596.2016.1220872>, 2017.

Ortiz-Monasterio R., J. I., Dhillon, S. S., and Fischer, R. A.: Date of sowing effects on grain yield and yield components of irrigated spring wheat cultivars and relationships with radiation and temperature in Ludhiana, India, *F. Crop. Res.*, 37, 169–184, [https://doi.org/10.1016/0378-4290\(94\)90096-5](https://doi.org/10.1016/0378-4290(94)90096-5), 1994.

Pleijel, H., Danielsson, H., Gelang, J., Sild, E., and Selldén, G.: Growth stage dependence of the grain yield response to ozone in spring wheat (*Triticum aestivum* L.), *Agric. Ecosyst. Environ.*, 70, 61–68, [https://doi.org/10.1016/S0167-8809\(97\)00167-9](https://doi.org/10.1016/S0167-8809(97)00167-9), 1998.

652 Pleijel, H., Eriksen, A. B., Danielsson, H., Bondesson, N., and Selldén, G.: Differential ozone sensitivity in an old and a modern  
653 Swedish wheat cultivar - Grain yield and quality, leaf chlorophyll and stomatal conductance, *Environ. Exp. Bot.*, 56, 63–71,  
654 <https://doi.org/10.1016/j.envexpbot.2005.01.004>, 2006.

655 Pleijel, H., Danielsson, H., Emberson, L., Ashmore, M. R., and Mills, G.: Ozone risk assessment for agricultural crops in  
656 Europe: Further development of stomatal flux and flux-response relationships for European wheat and potato, *Atmos. Environ.*,  
657 41, 3022–3040, <https://doi.org/10.1016/j.atmosenv.2006.12.002>, 2007.

658 Rathore, A., Gopikrishnan, G. S., and Kuttippurath, J.: Changes in tropospheric ozone over India: Variability, long-term trends  
659 and climate forcing, *Atmos. Environ.*, 309, 119959, <https://doi.org/10.1016/j.atmosenv.2023.119959>, 2023.

660 Riahi, K., Rao, S., Krey, V., Cho, C., Chirkov, V., Fischer, G., Kindermann, G., Nakicenovic, N., and Rafaj, P.: RCP 8.5-A  
661 scenario of comparatively high greenhouse gas emissions, *Clim. Change*, 109, 33–57, [https://doi.org/10.1007/s10584-011-](https://doi.org/10.1007/s10584-011-0149-y)  
662 0149-y, 2011.

663 Roy, S., Beig, G., and Jacob, D.: Seasonal distribution of ozone and its precursors over the tropical Indian region using regional  
664 chemistry-transport model, *J. Geophys. Res. Atmos.*, 113, 1–15, <https://doi.org/10.1029/2007JD009712>, 2008.

665 Roy, S. D., Beig, G., and Ghude, S. D.: Exposure-plant response of ambient ozone over the tropical Indian region, *Atmos.*  
666 *Chem. Phys.*, 9, 5253–5260, <https://doi.org/10.5194/acp-9-5253-2009>, 2009.

667 Ruane, A. C., Rosenzweig, C., Asseng, S., Boote, K. J., Elliott, J., Ewert, F., Jones, J. W., Martre, P., McDermid, S. P., Müller,  
668 C., Snyder, A., and Thorburn, P. J.: An AgMIP framework for improved agricultural representation in integrated assessment  
669 models, *Environ. Res. Lett.*, 12, <https://doi.org/10.1088/1748-9326/aa8da6>, 2017.

670 Rydsaa, J. H., Stordal, F., Gerosa, G., Finco, A., and Hodnebrog: Evaluating stomatal ozone fluxes in WRF-Chem: Comparing  
671 ozone uptake in Mediterranean ecosystems, *Atmos. Environ.*, 143, 237–248, <https://doi.org/10.1016/j.atmosenv.2016.08.057>,  
672 2016.

673 Sharma, A., Ojha, N., Pozzer, A., Mar, K. A., Beig, G., Lelieveld, J., and Gunthe, S. S.: WRF-Chem simulated surface ozone  
674 over south Asia during the pre-monsoon: effects of emission inventories and chemical mechanisms, *Atmos. Chem. Phys.*, 17,  
675 14393–14413, <https://doi.org/10.5194/acp-17-14393-2017>, 2017

676 Sharma, A., Ojha, N., Pozzer, A., Beig, G., and Gunthe, S. S.: Revisiting the crop yield loss in India attributable to ozone,  
677 *Atmos. Environ. X*, 1, 100008, <https://doi.org/10.1016/j.aeaoa.2019.100008>, 2019.

678 Sharma, A., C. Venkataraman, K. Muduchuru, V. Singh, A. Kesarkar, S. Ghosh, and S. Dey., Aerosol radiative feedback  
679 enhances particulate pollution over India: A process understanding, *Atmos. Environ.*, 298, 119609, doi:  
680 <https://doi.org/10.1016/j.atmosenv.2023.119609>, 2023

681 Shukla, K., Srivastava, P. K., Banerjee, T., and Aneja, V. P.: Trend and variability of atmospheric ozone over middle Indo-  
682 Gangetic Plain: impacts of seasonality and precursor gases, *Environ. Sci. Pollut. Res.*, 24, 164–179,  
683 <https://doi.org/10.1007/s11356-016-7738-2>, 2017.

684 Shuttleworth, W. J. and Wallace, J. S.: Evaporation from sparse crops-an energy combination theory, *Q. J. R. Meteorol. Soc.*,  
685 111, 839–855, <https://doi.org/10.1002/qj.49711146510>, 1985.

686 Singh, A. A. and Agrawal, S. B.: Tropospheric ozone pollution in India: effects on crop yield and product quality, *Environ.*  
687 *Sci. Pollut. Res.*, 24, 4367–4382, <https://doi.org/10.1007/s11356-016-8178-8>, 2017.

688 Steduto, P., Hsiao, T. C., Fereres, E., and Raes, D.: Crop yield response to water, *FAO Irrigation and Drainage Paper* no. 66,  
689 2012.

690 Stockwell, W. R., Middleton, P., Chang, J. S., and Tang, X.: The second generation regional acid deposition model chemical  
691 mechanism for regional air quality modeling, *J. Geophys. Res. Atmos.*, 95, 16343–16367,  
692 <https://doi.org/10.1029/JD095iD10p16343>, 1990.

693 Tai, A. P. K. and Martin, M. V.: Impacts of ozone air pollution and temperature extremes on crop yields: Spatial variability,  
694 adaptation and implications for future food security, *Atmos. Environ.*, 169, 11–21,  
695 <https://doi.org/10.1016/j.atmosenv.2017.09.002>, 2017.

696 Tai, A. P. K., Martin, M. V., and Heald, C. L.: Threat to future global food security from climate change and ozone air pollution,  
697 *Nat. Clim. Chang.*, 4, 817–821, <https://doi.org/10.1038/nclimate2317>, 2014.

698 Tans, P.P., Conway, T.J., n.d. Global means constructed using about 70 CMDL CCGG Sampling Network station data. [online]  
699 viewed 8 February 2020, available at: <https://data.giss.nasa.gov/modelforce/ghgases/Fig1A.ext.txt>.

700 Teixeira, E., Fischer, G., van Velthuisen, H., van Dingenen, R., Dentener, F., Mills, G., Walter, C., and Ewert, F.: Limited  
701 potential of crop management for mitigating surface ozone impacts on global food supply, *Atmos. Environ.*, 45, 2569–2576,  
702 <https://doi.org/10.1016/j.atmosenv.2011.02.002>, 2011.

703 Tripathi, A. and Mishra, A. K.: The Wheat Sector in India: Production, Policies and Food Security, in: *The Eurasian Wheat*  
704 *Belt and Food Security: Global and Regional Aspects*, 275–296, [https://doi.org/10.1007/978-3-319-33239-0\\_17](https://doi.org/10.1007/978-3-319-33239-0_17), 2017.

705 Tuovinen, J.-P., Ashmore, M. R., Emberson, L.D. and Simpson, D.: Testing and improving the EMEP ozone deposition model,  
706 *Atmos. Environ.*, 38, 2373–2385, <https://doi.org/10.1016/j.atmosenv.2004.01.026>

707 van Vuuren, D. P., Edmonds, J., Kainuma, M., Riahi, K., Thomson, A., Hibbard, K., Hurtt, G. C., Kram, T., Krey, V.,  
708 Lamarque, J. F., Masui, T., Meinshausen, M., Nakicenovic, N., Smith, S. J., and Rose, S. K.: The representative concentration  
709 pathways: An overview, *Clim. Change*, 109, 5–31, <https://doi.org/10.1007/s10584-011-0148-z>, 2011.

710 UNDESA (United Nations Department of Economic and Social Affairs), 2022. *World Population Prospects 2022: Summary*  
711 *of Results*. UN DESA/POP/2-22/TR/NO.3.

712 Wada, Y., Wisser, D., Eisner, S., Flörke, M., Gerten, D., Haddeland, I., Hanasaki, N., Masaki, Y., Portmann, F. T., Stacke, T.,  
713 Tessler, Z., and Schewe, J.: Multimodel projections and uncertainties of irrigation water demand under climate change,  
714 *Geophys. Res. Lett.*, 40, 4626–4632, <https://doi.org/10.1002/grl.50686>, 2013.

715 Wang, H. W., Li, X. B., Wang, D., Zhao, J., He, H. di, and Peng, Z. R.: Regional prediction of ground-level ozone using a  
716 hybrid sequence-to-sequence deep learning approach, *J. Clean. Prod.*, 253, 119841,  
717 <https://doi.org/10.1016/j.jclepro.2019.119841>, 2020.

718 Wilkinson, S. and Davies, W.J., Drought, ozone, ABA and ethylene: new insights from cell to plant to community, *Plant, Cell*  
719 *and Env.*, 33, 4, <https://doi.org/10.1111/j.1365-3040.2009.02052.x>, 2011.

720 Wu, S., Mickley, L. J., Leibensperger, E. M., Jacob, D. J., Rind, D., and Streets, D. G.: Effects of 2000–2050 global change  
 721 on ozone air quality in the United States, *Journal of Geophysical Research: Atmospheres*, 113, D06 302,  
 722 <https://doi.org/10.1029/2007JD008917>, 2008.

723 Yadav, D. S., Rai, R., Mishra, A. K., Chaudhary, N., Mukherjee, A., Agrawal, S. B., and Agrawal, M.: ROS production and  
 724 its detoxification in early and late sown cultivars of wheat under future O<sub>3</sub> concentration, *Sci. Total Environ.*, 659, 200–210,  
 725 <https://doi.org/10.1016/j.scitotenv.2018.12.352>, 2019.

726 Yadav, D. S., Mishra, A. K., Rai, R., Chaudhary, N., Mukherjee, A., Agrawal, S. B., and Agrawal, M.: Responses of an old  
 727 and a modern Indian wheat cultivar to future O<sub>3</sub> level: Physiological, yield and grain quality parameters, *Environ. Pollut.*, 259,  
 728 <https://doi.org/10.1016/j.envpol.2020.113939>, 2020.

729 Yadav, D. S., Agrawal, S. B., and Agrawal, M.: Ozone flux-effect relationship for early and late sown Indian wheat cultivars:  
 730 Growth, biomass, and yield, *F. Crop. Res.*, 263, 108076, <https://doi.org/10.1016/j.fcr.2021.108076>, 2021.

731 Yao, A. Y. M.: Agricultural potential estimated from the ratio of actual to potential evapotranspiration, *Agric. Meteorol.*, 13,  
 732 405–417, [https://doi.org/10.1016/0002-1571\(74\)90081-8](https://doi.org/10.1016/0002-1571(74)90081-8), 1974.

733 Zanis, P., Akritidis, D., Turnock, S., Naik, V., Szopa, S., Georgoulas, A.K., Bauer, S.E., Deushi, M., Horowitz, L.W., Keeble,  
 734 J. and Le Sager, P., 2022. Climate change penalty and benefit on surface ozone: a global perspective based on CMIP6 earth  
 735 system models. *Environmental Research Letters*, 17(2), p.024014

736 Zaveri, E. and Lobell, D. B.: The role of irrigation in changing wheat yields and heat sensitivity in India, *Nat. Commun.*, 10,  
 737 <https://doi.org/10.1038/s41467-019-12183-9>, 2019.

738 Zaveri, E., Grogan, D. S., Fisher-Vanden, K., Frolking, S., Lammers, R. B., Wrenn, D. H., Prusevich, A., and Nicholas, R. E.:  
 739 Invisible water, visible impact: Groundwater use and Indian agriculture under climate change, *Environ. Res. Lett.*, 11,  
 740 <https://doi.org/10.1088/1748-9326/11/8/084005>, 2016.

741

742